Worcester Polytechnic Institute
Chemical Engineering Department

Master of Science in Chemical Engineering

Thesis

PROTEIN PURIFICATION USING EXPANDED BED CHROMATOGRAPHY

Author : Fabien Ramat

Advisor: Professor William M. Clark

Department head: Professor Ravindra Datta

Winter 2004

<u>Acknowledgements:</u>

I would like to thank my advisor, Prof. William M. Clark, for his guidance, patience and enthusiasm concerning this work.

A special thanks to all the faculty and staff from the Chemical Engineering Department at Worcester Polytechnic Institute.

I would like to thank all the grad-students from our department as well as my roommates from 36 John Street that helped me through this journey and with who I had an enjoyable time in Worcester.

I would also thank my family that always supported me during my studies.

A special thank to the Worcester Rugby Football Club for their friendship and support.

Abstract

Expanded bed chromatography using ion-exchange media is a powerful first step in purification processes. Expanded bed chromatography can be used to extract components from complex and viscous solution. This can be achieved because of the void created between adsorbent particles where as in packed bed chromatography, the adsorbent is too compact and dense for a complex feed stock to flow through.

Expanded bed chromatography was used to purify bovine serum albumin (BSA) from chicken egg white (CEW). The high viscosity of CEW presents a unique challenge for efficient large-scale protein purification. This project aimed to optimize and evaluate a separation method that is believed to be particularly suitable for high viscosity solutions: expanded-bed ion exchange chromatography. The BSA was admixed into the CEW and the solution was pumped through the column for purification. The media used in the column was Streamline DEAE which is an anion-exchanger. The yield obtained was 85% and the purity was 57%.

A mathematical model to understand and predict the behavior of expanded bed chromatography was developed to provide an estimation of the breakthrough curves obtained for BSA.

A small sized porous dense adsorbent was also synthesized to enhance the purification process. This zirconia-based adsorbent allows use of higher flow velocities that is a key factor when working with viscous fluids such as chicken egg white.

<u>Keywords</u>: expanded bed chromatography, anion exchange, chicken egg white, protein purification, and zirconia.

Table of contents

List of Figures

List of Tables

1. Introduction

The completion of the human genome will lead to an unprecedented demand for the production of human proteins for diagnosing and treating disease and deficiencies. Recombinant DNA technology can provide for the large-scale production of human proteins using various host organisms (bioreactors) ranging from *E. coli* bacterial cells to transgenic farm animals. The newest form of recombinant bioreactor, the transgenic chicken bioreactor, is believed by many to be the nearly ideal host due to low costs for production and product isolation [1]. Transgenic chickens are being developed to produce large amounts of relatively easily recovered human proteins in the whites of their eggs [2].

In anticipation of the successful development of flocks of therapeutic protein producing transgenic chickens, this project aims to develop efficient separation methods for large-scale recovery of human protein from chicken egg white (CEW). In contrast to other recombinant protein production technologies that begin with large volumes of complex, dilute solutions that must be concentrated, CEW is a viscous, relatively concentrated, aqueous solution of about 15 proteins. The high viscosity of CEW presents a unique challenge for efficient large-scale protein purification. This project aims to optimize and evaluate a separation method that is believed to be particularly suitable for high viscosity solutions: expanded-bed ion exchange chromatography.

Bovine serum albumin was used as a model protein and mixed with fresh egg whites and subsequently recovered. Factors such as initial pretreatment and dilution that influence product recovery and product purity were investigated for expanded bed ion

exchange chromatography. A model to understand and predict the behavior of expanded bed chromatography was developed to provide a rational approach for developing commercial-scale purification methods for proteins from transgenic chicken eggs.

A small sized porous dense adsorbent was also synthesized to enhance the purification process. This zirconia based adsorbent allows use of higher flow velocities that is a key factor when working with viscous fluids such as chicken egg white.

2. <u>Background</u>

2.1. <u>Transgenic Chicken Eggs</u>

2.1.1. <u>Recombinant proteins</u>

Recombinant DNA technology has revolutionized the large-scale production of therapeutic proteins. In this technology, genes that control production of a protein from one organism, e.g. human insulin, are introduced into cells of another organism that are grown and coaxed into expressing the desired protein in a bioreactor. Engineered viruses are used as gene carriers. The ideal protein production system is one in which the host organism is easily and inexpensively grown and the desired protein is easily and inexpensively recovered in high purity and high yield. The three principal production methods used to date in the biotechnology industry, bacteria, yeast, and mammalian cells, have not reached this ideal [1]. Bacterial systems, such as *E. coli*, are easily grown and can obtain high protein yields but the purification costs are often high. Moreover, bacteria can not readily produce complex proteins that require post-translational modifications to be biologically active. Yeast systems, such as *Pichia*, are more complicated to grow than bacteria and are also limited to relatively simple proteins [3]. Mammalian cell culture systems can produce complex proteins, but are difficult to grow, have very low yields, and have extremely high production costs. These limitations together with an ever-increasing demand and market potential for human protein pharmaceuticals have prompted the recent development of transgenic plants and animals as whole-organism bioreactors.

Transgenic plants, grown in the same way as normal plants on a farm, can be made to produce therapeutic proteins in their roots, fruit, or leaves, but challenges remain

in terms of post-translational modifications and production costs. Figure 1 shows the cost for production and recovery for various hosts and bioreactors. Transgenic farm animals including cows, sheep, goats, and even pigs have been genetically engineered to produce recombinant products in their milk. The mammary gland is an efficient production vessel for complex proteins, but limitations with transgenic dairy animals include high purification costs in recovering a dilute product from a large volume of milk, high keeping costs, and long generation times to produce each recombinant animal. The newest form of recombinant bioreactor, and one believed by many to be the best, is the transgenic chicken bioreactor [4]. Although, the technology is not yet fully developed, it is expected that recombinant protein production in chicken eggs will soon be an important component of the biotechnology industry. Biotechnology companies in the United States pursuing this technology include AviGenics (Athens, GA), Origen Therapeutics (San Francisco, CA), GeneWorks (Ann Arbor, MI) and TransXenoGen (Shrewsbury, MA).
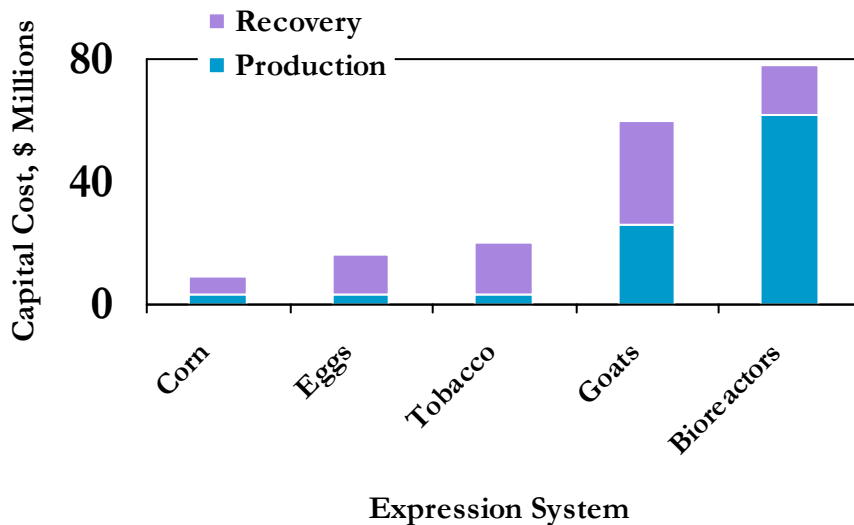
Figure 1 : Capital costs for production and recovery of recombinant proteins from various hosts [5].

The main advantage for recombinant chickens is that they can be bred and grown faster and with less expense than dairy animals, and with much less capital and operating cost than traditional cell culture techniques. Chickens start producing eggs 6 months after hatching and lay 21 eggs per month. Moreover, chickens are prolific egg producers and each egg white contains about 3 grams of protein. In comparison, goats, take 18 months from the creation of founder transgenic embryos to the production of milk by progeny [41]. The biochemical complexity of milk complicates the purification of recombinant proteins, and evolutionary conservation between humans and other animals means that many pharmaceuticals may adversely affect the production animal. Chickens can also tolerate proteins that would be toxic to animals such as goats. This is because aviaris and mammals diverged during evolution and developed different systems to handle proteins. Moreover, chickens can be contained in barns that can be controlled for cleanliness and disease. Goats, sheep need to roam fields where it is more difficult to control environmental factors. The expected ability to genetically engineer the eggs to contain as much as 0.5 grams of recombinant protein per egg represents a dramatic increase in production over that of conventional bioreactors and dairy animals. AviGenics estimates monoclonal antibody production costs per gram to be $100, $2-20, and $0.1-0.25 in cell culture, transgenic goats, and recombinant chicken eggs, respectively [2]. These production costs do not consider the protein recovery and purification costs which are also believed to be less for chicken eggs because of the comparatively less complex environment and expected initial high protein concentration in the egg compared to the other production systems. Figure 1 shows that production

costs are high for bioreactors and mammals such as goats whereas recovery costs are essentially the same for recombinant proteins produced in eggs or bioreactors.

2.1.2. Human serum albumin (HSA)

HSA has a molecular weight of 66,500 and an isoelectric point of 4.9. Its primary function is to maintain osmotic pressure within blood vessels. It also acts as a carrier for several molecules in the bloodstream including bilirubin and fatty acids. Large quantities of HSA are administered clinically in the treatment of blood loss due to surgery, shock, burn, or hypoproteinemia. HSA is currently produced primarily by recovery from human blood despite the high cost, variable availability, and danger of contamination by viruses, such as hepatitis, inherent in this method. Recently a method has been developed to produce HSA in recombinant *Pichia pastoris* [3,6]. As shown by the number of companies trying to synthesize this protein, there are considerable research efforts aimed at the production of human serum albumin in transgenic chicken eggs.

In our experiments, we will use bovine serum albumin because it is less costly that HSA and has chemical and physical properties close to those of HSA. Its molecular weight is 66,000 and its isoelectric point is 4.7.

2.1.3. Chicken egg white

Chicken egg white is a viscous aqueous solution with pH of 9.7, conductivity of 7.5 ms/cm and containing about 10 % protein by weight [7]. An egg contains 6.5g of proteins, and 3.6g of the total protein is egg white, of which 90% is accounted by seven genes; the ovalbumin gene alone accounts for 2 grams of egg white protein. As can be seen in Table 1 [8], there are about 15 different proteins in this mixture with

the most prominent being ovalbumin, ovotransferrin, ovomucoid, and lysozyme. The high viscosity is largely due to the very high molecular weight protein ovomucin. Egg white solutions behave as pseudoplastics since their viscosity decreases with increasing shear rate [7].

Table 1 : Composition and protein properties in chicken egg white.

	% of total	Isoelectric point	Molecular weight
Ovalbumin	54	4.5	45,000
Ovotransferrin	12	6	77,700
Ovomucoid	11	4.1	28,000
Lysozyme	3.4	10.7	14,300
Ovomucin	3	4.7	220,000
G3 Ovoglobulin	1	4.8	50,000
G2 Ovoglobulin	1	5	47,000
Ovoglycoprotein	1	3.9	24,400
Ovoflavoprotein	0.8	4	32,000
Ovomacroglobulin	0.5	4.5	900,000
Avidin	0.05	10	68,300
Cystatin	0.05	5.1	12,700
Thiamin-binding protein	N.D.	N.D.	38,000
Glutamyl aminopeptidase	N.D.	4.2	320,000
Minor glycoprotein 1	N.D.	5.7	52,000
Minor glycoprotein 2	N.D.	5.7	52,000

Human serum albumin	N.A.	4.9	66,500
Bovine serum albumin	N.A.	4.7	66,000

2.2. General information on bioseparations processes

Production of protein by genetically engineered microorganisms, yeast and animal cells has become a very important technique for the production of pharmaceuticals. The separation of recombinant proteins is a challenge due to the wide range of physical and chemical properties of the raw material. The feedstocks from which proteins are prepared are usually very complex and contain solid and dissolved biomass of various sizes and molecular masses. The desire to obtain a pure and defined substance of guaranteed purity and potency may not be achieved with a single purification step but with a combination of different unit operations as shown in Figure 2 [9].

The target protein may be either accumulated at the interior of cells or excreted. Whether accumulated or excreted, the first step in a purification protocol is clarification of either the cultivate broth or the cell homogenate. Microfiltration and centrifugation are commonly used for the separation of solids and soluble components. When working with centrifuges employed for large scale processes, centrifugation is done twice and followed by a microfiltration step.

Diluted product feedstocks often require a concentration step by ultrafiltration. An adsorption step with an ion-exchanger, can also be used because it has the advantage to yield partial purification and concentration simultaneously [9].

Expanded bed chromatography allows to integrate solid-liquid separation, volume reduction by protein adsorption and partial purification in one unit operation without compromising on separation efficiency, but saving considerably processing time and capital investment [10]. This process is based on the use of particulate adsorbents with different selectivities, which reside in a column system.

Accumulation of
products in cells

Cell Harvest

Excreted
Products

Release through
cell disruption

Solid-Liquid
Separation
- Centrifugation
- Microfiltration
Concentration
Primary Separation
- Adsorption

Expanded Bed
Chromatograph

*Primary
Separation*

Purification
- Chromatography

Polishing, Formulation

Product

*High-
resolution
Techniques*
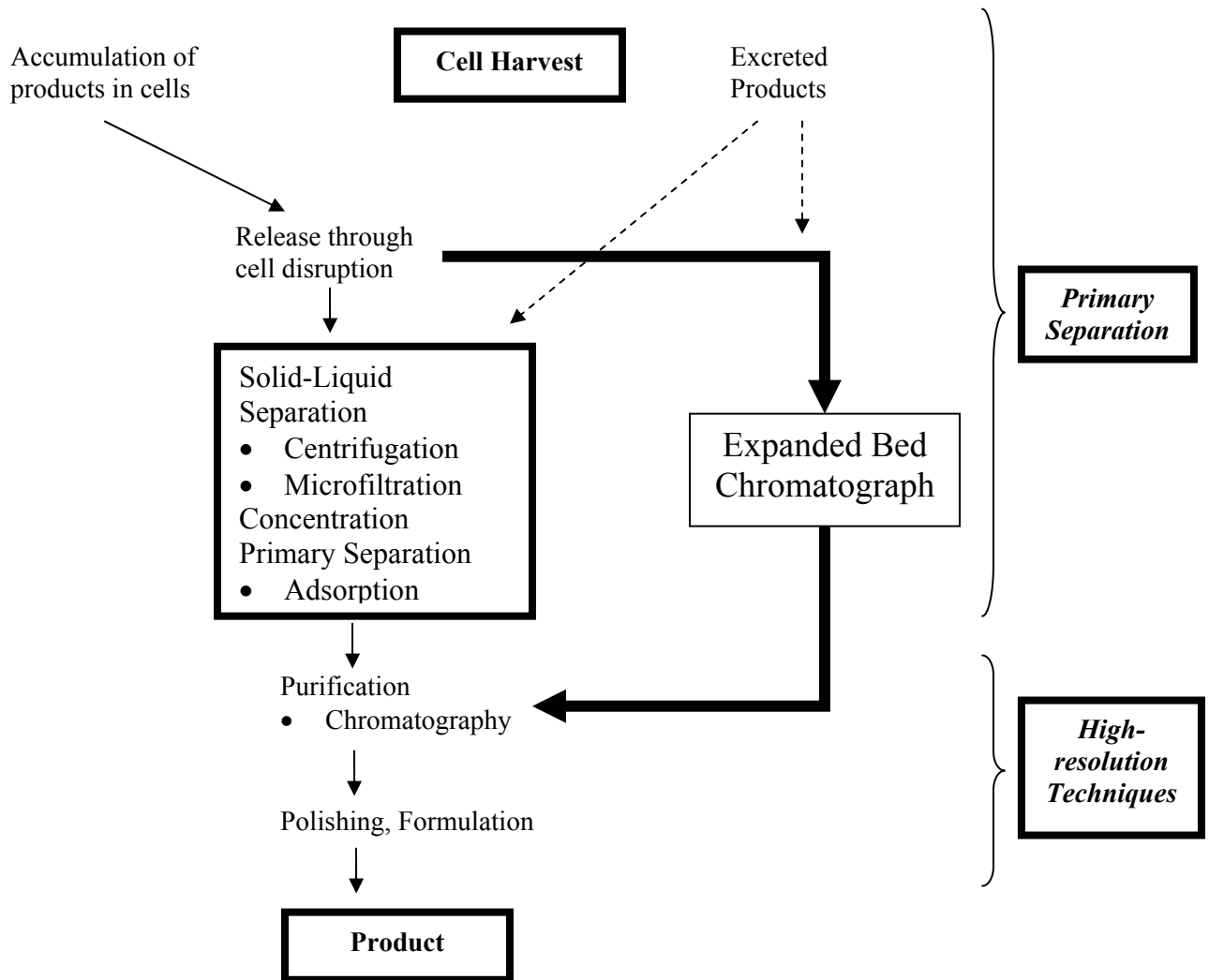
**Figure 2 : Role of expanded bed chromatography within a typical protein recovery
process [9].**

2.3. Previous studies regarding chicken egg white (CEW)

With the importance of chicken egg components rising, various methods have been developed for purification of different egg proteins in a minimum number of steps [8]. Major proteins have been separate by stepwise addition of ammonium sulfate and ion-exchange techniques using carboxymethyl cellulose and diethylaminoethyl cellulose [7]. Gel permeation and electrophoresis were also adopted for this purpose among other methods. However, no method for the complete isolation of all the proteins has been determined. Since large process volumes require large processing equipment and drive up process cost, some attempts have been made to reduce process volume. Expanded bed chromatography has been investigated for this purpose because it does not require a dilute feed like other chromatographic methods do [11].

Due to its low cost, easy scale-up and reversible binding properties, ion-exchange medias are commonly used in downstream processing of proteins. Anion-exchange chromatography offers the most complete analysis of all the egg proteins [8] as compared to gel permeation and reverse-phase chromatography.

2.3.1. *Awadé and A.L. [8]*

In this work, three chromatographic methods for the analysis of egg white proteins are studied: anion-exchange HPLC, reversed-phase HPLC and gel permeation chromatography. Although the samples are diluted to about eleven-fold, this work gives a precise idea of the performances of those techniques in terms of resolution; kind and

numbers of fractions recovered, and yield. Anion-exchange gives the best resolution and the recovery of the protein of interest was the highest. The elution sequence of the egg white proteins closely reflected the order of their isoelectric points, with the exception of lysozyme. Reversed-phase chromatography only fractioned eight peaks as compared to eleven by ion exchange. Moreover, 30% of the ovalbumin was retained in the column after elution in reverse phase. Finally, gel permeation should be recommended for ovomucin separation and reverse phase HPLC would be preferable for an accurate estimation of lysozyme and ovotransferin since with anion-exchange, these proteins are slightly contaminated with other minor proteins.

2.3.2. *Owen and Chase [12]*

This work aims at developing a continuous method for recovering lysozyme from unclarified chicken egg white using counter-current expanded bed adsorption. Although the feedstock was very diluted (1mg/ml) of dried egg whites, this work illustrates the use of expanded-beds for purifying unclarified egg-white components. An overall yield of 90.5% was obtained for lysozyme with a purification factor of 19.4 based on the initial unclarified feedstock. The final product stream was fully clarified. Although the authours claim that there is no need for pretreatment of crude sample, chicken egg white was obtained as a uniform powder which adds to the overall process cost. Also, the sample was highly diluted so that abnormal expansion of the beds due to high viscosity of a concentrated feedstock was negligible.

2.3.3. *Wright and Muzzio [13]*

They investigated the effect of viscosity on mass transfer in packed beds by estimating the reduction in mass transfer coefficient. This is the only work aimed at evaluating resistances in packed beds and expanded beds at different viscosity. Batch uptake of lyzozyme was investigated at theses viscosities for two different resins used for expanded-bed adsorption. To understand the limitations and mechanisms for the uptake, pore diffusion and homogeneous diffusion model were used, with the adsorption kinetics described by a linear isotherm of the Langmuir type. It was concluded that film mass transfer was dominant at higher viscosity in Streamline SP, a commercially available resin used in expanded bed adsorption. Intraparticle mass transfer dominated at lower viscosity.

2.3.4. *Tong and Dong [14]*

Lysozyme adsorption and purification from chicken egg white by expanded bed chromatography with a Nd-Fe-B alloy-densified agarose adsorbent modified with Cibacron Blue 3GA were investigated. The results were compared with a Cibacron Blue 3GA-modified Streamline gel. The chicken egg white solution was 30% (v/v) diluted and filtered before being injected in the column. The custom made adsorbent offered a higher density (1.88 mg/ml compared to 1.2 mg/ml) and a smaller size particle (mean diameter of 102 μm compared with 200 μm). The writers claim to have reduced the axial dispersion with their Nd-Fe-B adsorbent. But the purification performances are not

significant with the new adsorbent. Moreover, the modeling as well as the breakthrough curves do not seem realistic.

2.4. Ion-exchange chromatography

2.4.1. *Isoelectric point*

Every protein is characterized by its isoelectric point. The charge of a protein is decided by the pH of the solution: when the pH is equal to the isoelectric point, the protein carries no net charge. When the pH is greater than the isoelectric point (pI), the protein is negative and vice versa [16].

2.4.2. *Principles*

Proteins bind to ion exchangers by electrostatic forces between the adsorbent charged beads and the charged groups of the protein. The charges need to be balanced by counterions such as metal ions, chloride ions and sometimes, buffer ions. A protein has to move the counterion to be attached; the net charge of the protein will usually be the same as the counterions displaced. That is why this type of chromatography is called "ion-exchange". The proteins in solution are neutralized by the counterions such as Tris. As shown on Figure 3, a negative protein A is surrounded by $HTris^+$ ions and is entering a typical diethylaminoethyl (DEAE) adsorbent. The positive ligands in the DEAE are in equilibrium with negative Cl^- ions. The protein displaces those Cl^- ions to occupy a site in the adsorbent. TrisCl is discharged. The discharge of TrisCl increases the ionic strength of the buffer and can also change the pH. It is then recommended to use a small protein concentration and a small buffer concentration [16].

2.4.3. *Elution of the proteins*

In theory, two methods can be used for eluting proteins: modifying the pH of the buffer to a value where the binding is weaker or increasing the ionic strength of the buffer to weaken the electrostatic interactions between protein and adsorbent.
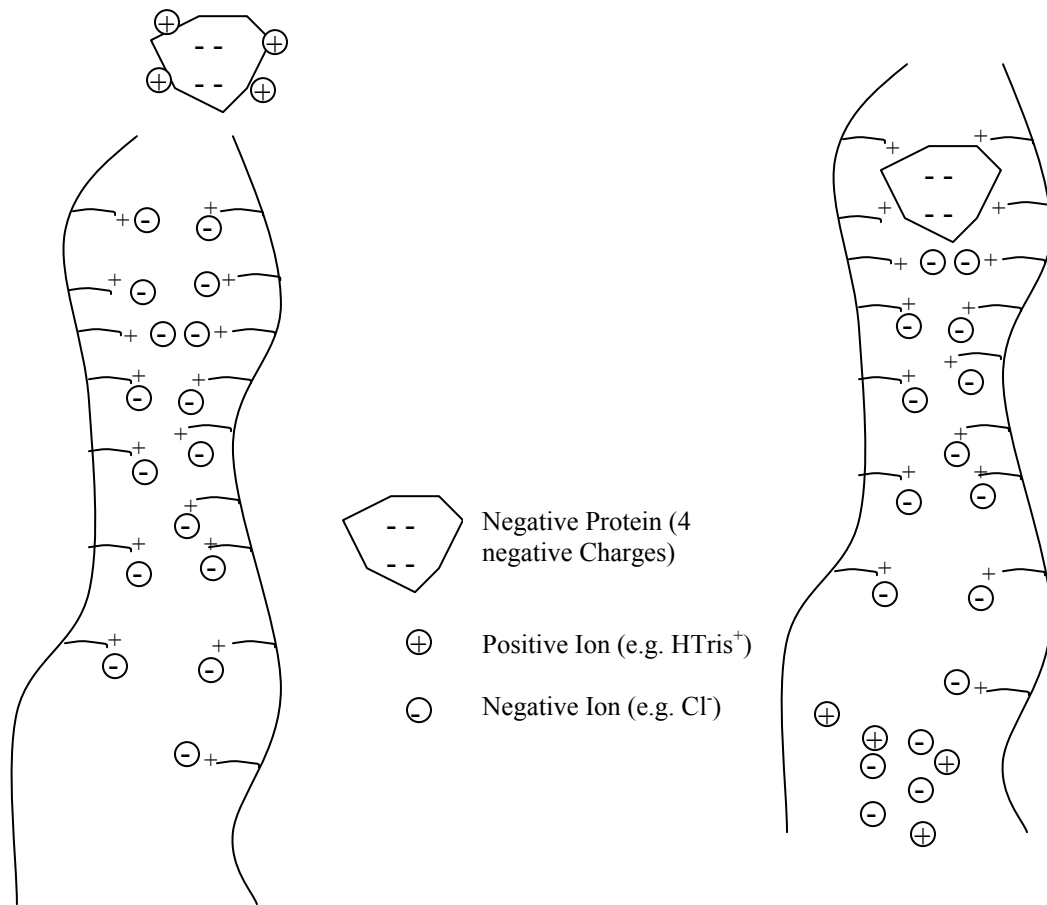
Figure 3 : Ion-exchange media when a negatively charged protein (surrounded with the positive counter ions) adsorbs to an anion exchanger. Four positive ions associated with the proteins are displaced with four negative ions from the exchanger [1.6].

The second method is more successful than increasing the pH of the solution. In practice, the ionic strength is increased by adding sodium chloride (NaCl) to the buffer. In order to determine the salt concentration to use to elute a certain protein, experiments with small (1ml) packed bed chromatography column were carried out. Packed bed columns are easy to use and only need small sample volume and reduced elution volume. Moreover, those experiments can be done on a shorter time scale than for expanded bed: there is no expansion and the cleaning in place procedure is very easy. The packed bed column needs to have the same kind of packing, the same type of ligand as in the one used in the expanded bed in order to predict the behavior of the expanded bed adsorbent.

2.5. Expanded bed characteristics

2.5.1. *Basic principles on expanded bed chromatography*

2.5.1.1. *Principles of operation*

In expanded bed chromatography, viscous and particulate-containing feeds that would foul a traditional packed column are accommodated by introducing the feed upward through a column packed with media designed to be suspended and dispersed in the upward flow. The bed expansion creates an increased void space between adsorbent particles allowing passage of particulate contaminants in the feed and preventing unacceptable pressure buildup within the column. Once the feed is loaded and the target product is bound to the adsorbent, a wash step is performed, also in expanded bed upward flow mode, to remove particulates and unbound contaminants. Elution of the target product is then performed via downward flow in traditional packed bed mode. Some studies relate elution performed with an expanded bed upward flow mode [14]. This tends to increase the elution volume. A clean-in-place procedure is normally required after elution to prepare the column for another loading step [15].

An expanded bed is essentially a cross between a packed bed, with stationary particles and low fluid dispersion, and a fluidized bed, with randomly mixing particles and high fluid dispersion [9]. Process design variables for optimizing expanded bed chromatographic separations include chemical and physical properties of the packing media and of the feed solutions. Chromatographic media with the appropriate density, particle size distribution, and mechanical stability required for expanded bed operation are commercially available with several different chemistries including anion and cation

exchange.   The chemical properties of the feed such as pH, ionic strength, and buffer type that affect selectivity and capacity of the process have essentially the same effect in expanded bed mode as they do in traditional packed bed chromatography.

2.5.1.2.Column requirements

The major differences with a packed bed column are the two adaptors. The bottom adaptor has to be specially designed to ensure a perfect plug flow through the column. Usually, the flow through a packed bed column creates such a high pressure drop that it assists the adaptor to generate a plug flow through the column. The pressure drop being low in an expanded bed, the plug flow has to be created with the adaptor only. Therefore, the bottom adaptor needs to create a pressure drop and to ensure a perfectly vertical flow – a radial direction would cause turbulence that propagates in the column. The flow distributor is usually a bed glass of ballotini or, in our column, a plate with holes. The two stainless steel plates used contain six 1mm or 0.5mm diameter holes placed in a hexagonal manner. The distributor plate enables the passage of particulates without a blockage. To prevent the adsorbent from leaving the column, a 50μm mesh size stainless steel net is positioned above the metal plate. The size mesh of the screen must be lower than the size of the adsorbent particle. Finally, to have a sanitary design, there must be no stagnant zones where cells, particles or debris can accumulate.

Figure 4 describes the different adaptor as well as the hydraulic piston. Zone 1 is filled with water to control the height of the upper adaptor and the adsorbent is located is what we called zone 2. The upper adaptor allows using an upward flow or a downward flow (i.e. elution of protein in packed bed mode). The upper adaptor needs to be able to

move in order to operate in both expanded and packed bed. This can be done manually or, in our set-up, hydraulically. The adaptor is lowered when filling zone 1 (Figure 4) with water and allowing the liquid to go through the bottom adaptor. It is moved up by closing the outlet of the column (i.e. the top adaptor) and using upward flow through the bottom adaptor. Therefore, zone 1 is used to monitor the height of the column where zone 2 is the adsorption zone. The column has to be placed in a perfect vertical alignment to ensure the stability of the bed.
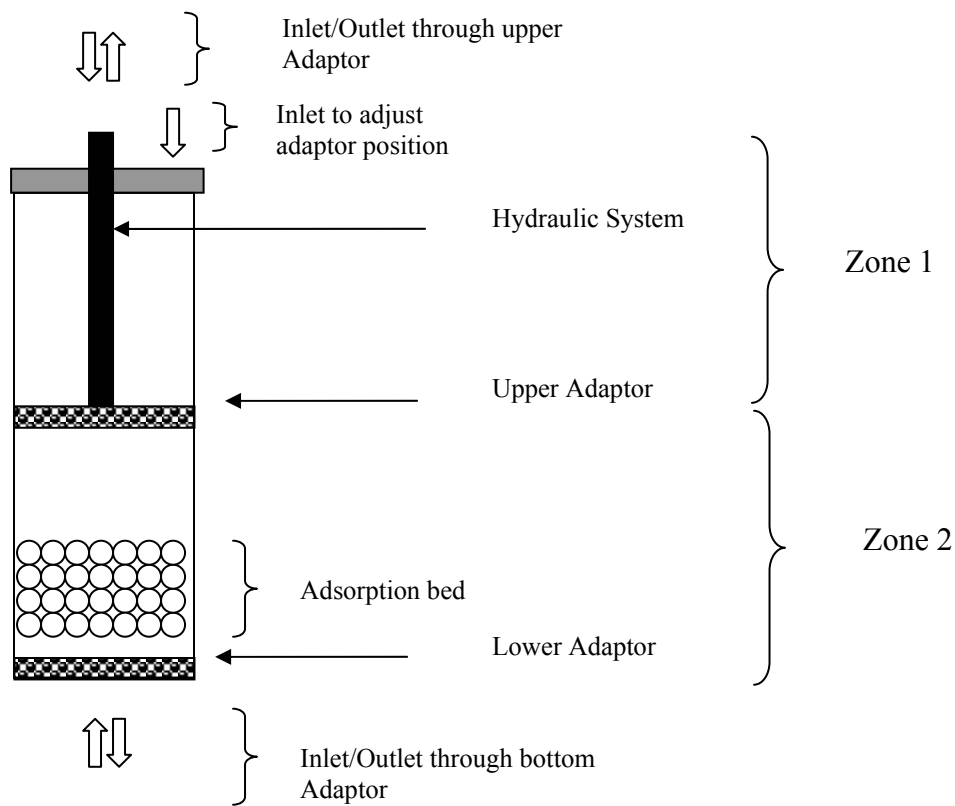
Figure 4 : Column description

2.5.1.3. *Elution in expanded bed mode*

Even though elution in expanded bed mode requires a greater quantity of solvent, we used this method because it is easier to elute proteins contained in a viscous solution. Elution in packed bed mode, where the upper adaptor is lowered to the sedimented bed height, is also available. In packed bed mode, where the column is used as a packed bed column in fact, the elution can be done with a downward flow.

The principle of elution in expanded bed mode is described in Figure 5 where NaCl is used as the molecule that decreases the bound between the proteins and the adsorbent.

Non-binding protein collected	First desired protein collected	Second desired protein collected

Equilibration Step with buffer	Sample injection	First elution with $[NaCl]_0$	First elution with $[NaCl]_1 > [NaCl]_1$
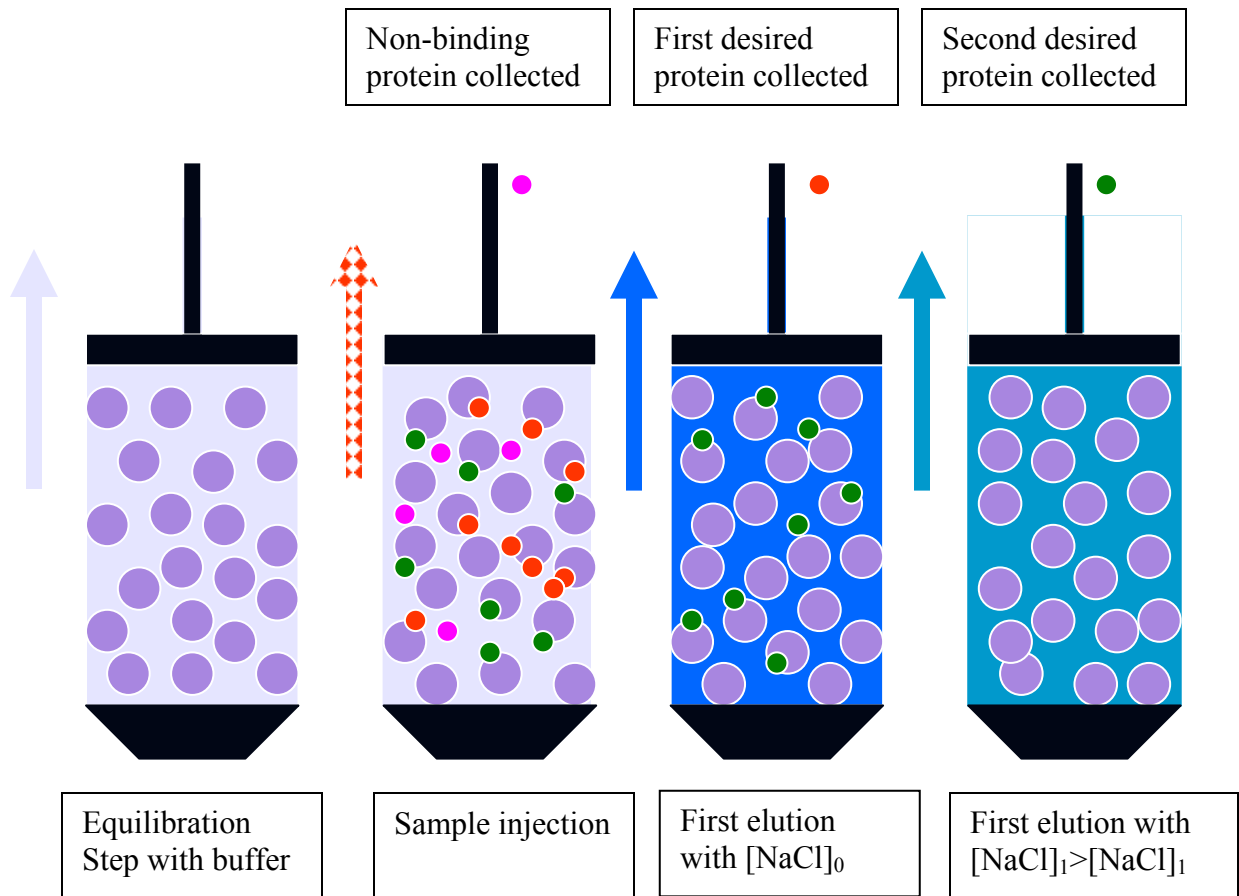
Figure 5 : Principle of elution in expanded bed mode

2.5.2. _Bed expansion_

The bed expansion α is calculated as the ratio between the expanded bed height (H) and the sedimented bed height (H_0).

$$\alpha = \frac{H}{H_0} \qquad (1.1)$$

2.5.3. _Axial dispersion_

The Bodenstein number was used to calculate the axial dispersion coefficient D_{ax} [10]. The Bodenstein number is the ratio of convective to dispersion mass transport as defined in Equation 1.2. It relates dispersed flow (D_{ax}) to convective flow ($uH\varepsilon^{-1}$). Bo can be determined from the variance by using Equation 1.3, [17]. The variance can be determined from the residence time distribution (RTD) analysis and the short-cut method [18,19] explained below.

$$Bo = \frac{uH}{\varepsilon Dax} \qquad (1.2)$$

$$\sigma_\theta^2 = \frac{2}{Bo} + \frac{8}{Bo^2} \qquad (1.3)$$

where u is the superficial fluidizing velocity, ε the bed voidage and σ_θ the dimensionless variance.

The average bed voidage ε can be estimated from the following formula [18]:

$$\varepsilon = 1 - (1 - \varepsilon_0) . \frac{H_0}{H} \qquad (1.4)$$

The settled bed voidage ε_0 is often assumed to be 0.418 [20]. When the Bodenstein number is greater than 40, axial mixing has little effect on the adsorption performances. It behaves similarly to a packed bed [9]. Bo increase with the height of the sedimented bed. A decrease of the Bodenstein number during the operation indicates that the expansion is disturbed by particle aggregating or local turbulence in the column. The sedimented bed must have a minimal height for efficient protein adsorption otherwise dispersion is limiting (Bo<40) and a high percentage of the target protein will be lost in early breakthrough fraction.

2.5.4. *Fluidization characteristics*

The Richardson-Zaki correlation [21] describes the effects of bed voidage on the rate of settling and allows prediction of the liquid velocity required to produce a given degree of expansion during fluidization. The correlation is confined to uniformly sized, non-porous, spherical particles greater than 100 μm in diameter with the same density. Even though it is not suitable for modeling particle mixing, it is usually used to predict and model the expansion behavior of expanded-bed adsorption column. Following the approach of Richardson and Zaki [21], the terminal velocity u_t can be determined from Stokes' Equation (Equation 1.5). The particle Reynolds number, Re_p, at the terminal settling velocity is calculated using Equation 1.6 and used to determine which Equation should be used for the expansion index n [18,19].

$$U_t = \frac{(\rho_p - \rho_l).d_p^2.g}{18\eta}$$		(1.5)
$$Re_t = \frac{u_t.d_p.\rho_l}{\eta}$$		(1.6)
$$n = 4.65 + 19.5\frac{d_p}{d_c}$$	$Re_t < 0.2$	(1.7.1)
$$n = (4.35 + 17.5\frac{d_p}{d_c}).Re^{-0.03}$$	$0.2 < Re_t < 1$	(1.7.2)
$$n = (4.45 + 18\frac{d_p}{d_c}).Re^{-0.1}$$	$1 < Re_t < 500$	(1.7.3)

Where d_p is the particle diameter, d_c that of the column, η the liquid viscosity and ρ_l the liquid density.

In the majority of cases, it is assumed that the diameter of the particle is much smaller than that of the column ($d_p/d_c < 0.01$) where wall effects are not significant and also that values of Re_t satisfy $Re_t < 0.2$ where laminar liquid flow around the particle occurs.

The bed expansion index can therefore be calculated using the adequate equation. By solving Equation 1.8, we can obtain the bed voidage. Equation 1.9 leads us to the predicted height of the bed. To test the validity of the Richardson-Zaki correlation, Equations 1.8 and 1.9 can be fitted to experimental data. u_t and n can be determined by plotting log(u) as a function of log(ε) [22].

$$u = u_t.\varepsilon^n$$	(1.8)
$$H = H_0 \frac{1 - \varepsilon_0}{1 - \varepsilon}$$	(1.9)

2.5.5. *Number of theoretical plates*

An efficient way to measure the column efficiency is by calculating the height equivalent to a theoretical plate (HETP) under certain operating conditions. The smaller the HETP, the more efficient the column is in terms of resolution and product concentration.

Van Deemter proved that the HETP is a function of the superficial velocity (u) [23]:

$$HETP = A + \frac{B}{u} + Cu \qquad (1.10)$$

A accounts for the dispersion, B for the molecular diffusion and C for the intraparticle effects [24]. The molecular diffusion is usually negligible in protein chromatography. The most significant effects comes from the intraparticle effects (film mass transfer resistance; adsorption/desorption rates). HETP can be reduced by decreasing the particle size and by using non-porous adsorbent. However, the decrease of size particle will increase the pressure drop to an unacceptable level and the use of non-porous particle will decrease the adsorption capacities of the adsorbent. Macroporous particle that allow intraparticle convection help reduce mass transfer resistances and have been shown to exhibit a plateauing of the HETP curve with velocity, therefore providing a small value of HETP even for high velocity [25]. While macroporosity ensures intraparticle convective flow, small and heavy particle permits small diffusion lengths and higher

interstitial bed expansion velocities, respectively. This would give an efficient and stable expanded bed.

HETP is calculated using the Residence Time Distribution (RTD). The RTD test is a tracer stimulus method that can be used to assess the degree of longitudinal axial mixing (dispersion) in the expanded bed by defining the number of theoretical plates. A 1% (V/V) acetone solution is used as the tracer input into the fluid entering the column. The number of theoretical plates is calculated from the mean residence time of the tracer and the variance of the tracer output signal, representing the standard band broadening of a sample zone.

Here is the procedure used to calculate the number of theoretical plates and the HETP [15,18,19]:

1 – Fully expand the bed at the desired velocity

2 – Lower the adaptor to 0.5 – 1 cm above the expanded bed surface

3 – Change to the acetone-buffer solution until the UV signal reaches a plateau

4 – Change back to the equilibration buffer and mark the time.

5 – Wait until the signal reaches the baseline level.

The number of theoretical plates is calculated using:

$$N = \frac{t_r^2}{\sigma^2}$$

(1.11)

where t_r is the mean residence time and sigma the standard deviation. t_r is the distance from the mark (step 4 of the procedure) to the 50% of the maximum UV signal. σ is measured as half the distance between the points 15.85% and 84.15% of the maximum UV-signal as shown in Figure 6. The value of the HETP is obtained using:

$$HETP = \frac{H}{N} \qquad (1.12)$$

where H is the height of the expanded bed.

If the mean residence time calculated as above is significantly shorter than the theoretical residence time (hydrodynamic residence time calculated from the reactor volume and the applied flow rate), it indicates an insufficient fluidization and the formation of flow channel in the lower part of the bed, causing early breakthrough of the buffer front.
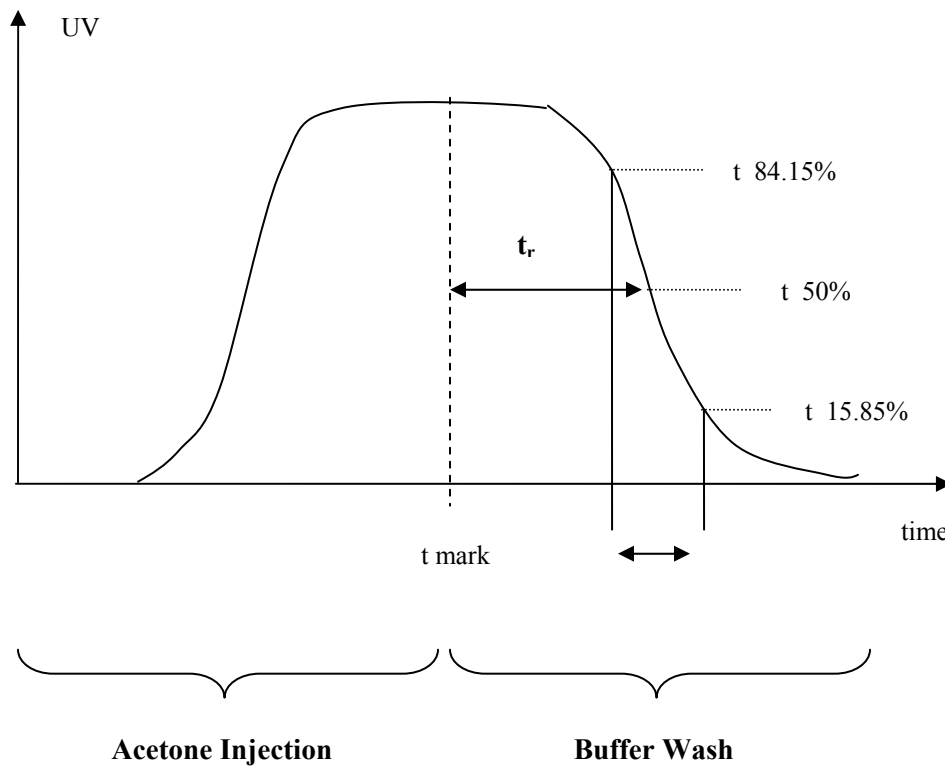
Figure 6 : Calculation of the mean residence time and the variance using the RTD.

2.6. Dynamic binding capacity

2.6.1. *Breakthrough curve*

The concentration profile at the output of the column to a step-like response would be as shown in Figure 7 if the following assumptions held [26]:

1. external and internal mass-transfer resistance negligible

2. plug flow is achieved

3. axial dispersion is negligible

4. the adsorbent is initially free of adsorbent

5. the adsorption isotherm begins at the time origin and the equilibrium between the fluid and the adsorbent is achieved instantaneously
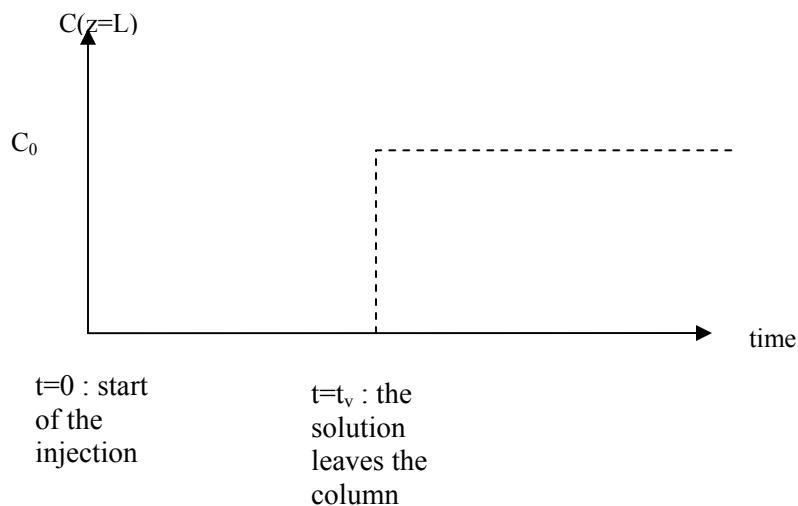
Figure 7 : Ideal breakthrough curve

At t=0, the sample with a concentration C_0 is injected in a step-like manner. Until t_v, the adsorbent is being saturated with adsorbate and the concentration of the solute in the fluid is that of the feed, C_0. Between t=0 and t=t_v, in the upstream region of the column, the

adsorbent is spent, where in the downstream region, the concentration of the fluid is zero and the adsorbent is free of adsorbate. When the whole adsorbent is spent (at t_v), the concentration of the solute in the fluid abruptly rises to the inlet concentration C_0 (Figure 7) ; no further adsorption is possible.

In a real chromatography column, the profile shown in Figure 7 is not valid. Internal transport resistance and external transport resistance are finite. Axial dispersion can be significant, especially in an expanded bed. These factors contribute to the development of broader concentration profiles such as shown in Figure 8.
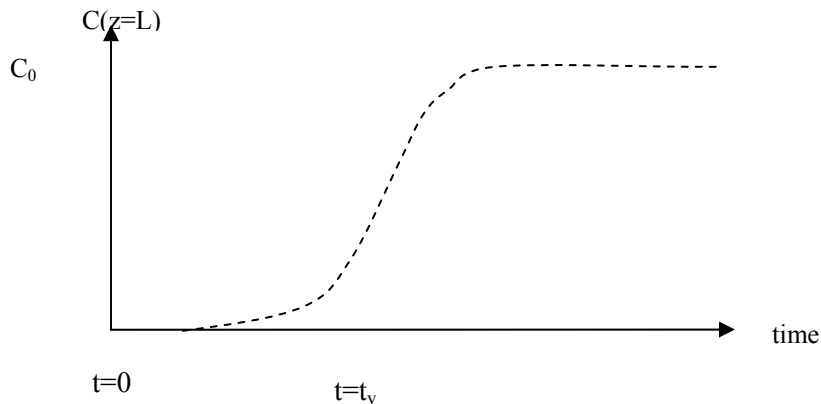
Figure 8 : Actual breakthrough curve

This type of curve is called a 'breakthrough curve'. In order to obtain those curves, we only use one protein under binding conditions.

2.6.2. *Dynamic binding capacity*

The dynamic binding capacity is defined as the total amount of a certain protein in the column subtracting the amount in the dead space per unit adsorbent volume. The dead space is located between the height of the bed and the upper adaptor. The quantity of protein in this space is denoted by Q_d (in mg).

The dynamic capacity is calculated when the outlet concentration is equal to 40% of the feed concentration. The quantity of protein is $Q_{40\%}$ (in mg). The method of Griffith is used [10] :

$$Q_{40\%} = u.C_o . \int_{t=0}^{t(c/Co=0.4)} (1 - \frac{c}{C_0})dt$$	(1.13)
$$Q_d = V_d . C_0$$	(1.14)
$$DBC = \frac{Q_{40\%} - Q_d}{Vs}$$	(1.15)

where:

C_0: protein concentration in the feed solution (mg/ml)

u: the flow rate (ml/h)

V_d: the dead volume between the height of the bed and the upper adaptor (ml)

V_s: the sedimented bed volume (ml of adsorbent)

2.7. <u>Modeling the behavior of expanded-bed chromatography</u>

In order to understand the behavior of the column, the mass-transfer effects for homogeneous diffusion and the pore diffusion models were solved to understand the effects on mass-transfer mechanism and intraparticle mass-transfer resistance as functions of hydrodynamic factors.

2.7.1. *Liquid phase*

In the liquid phase, only is taken into account the proteins that between z and z+dz, do not bind to the solid adsorbent particle.

The mass balance with respect to the liquid phase is described as follows:

Bulk flow *in* at (z) + Dispersion *in* at (z) = Accumulation in the liquid between (z) and (z+dz) + Bulk flow *out* at (z+dz) + Dispersion *out* at (z+dz) + mass transfer to solid phase between (z) and (z+dz).

In a mathematical manner:

$\varepsilon_L A u(z) C(z) - Dax \varepsilon_L A \dfrac{\partial C}{\partial z}\bigg|_z = \varepsilon_L \dfrac{\partial C}{\partial t} A dz + \varepsilon_L A u(z+dz) C(z+dz)$	(1.16.1)
$- Dax \varepsilon_L A \dfrac{\partial C}{\partial z}\bigg|_{z+dz} + \dfrac{3 k_f \varepsilon_s}{R_p}\left(C - C_f\right) A dz$	

It has to be noticed that the derivative of the concentration over the axial coordinate is negative.

Rearranging (1) gives:

$\dfrac{\partial C}{\partial t} = Dax \dfrac{\partial^2 C}{\partial z^2} - \dfrac{\partial u C}{\partial z} + \dfrac{3 k_f \varepsilon_s}{\varepsilon_p R_p}\left(C - C_f\right)$	(1.16.2)

Assuming that the linear velocity remains constant throughout the column leads to:

$$\frac{\partial C}{\partial t} = Dax \frac{\partial^2 C}{\partial z^2} - u \frac{\partial C}{\partial z} + \frac{3k_f \varepsilon_s}{\varepsilon_p R_p} \left(C - C_f\right)$$

(1.17)

The initial concentration is considered to be zero (Initial Condition IC):

$$C(z, t = o)$$

(1.17.1)

The first boundary condition shows the effect of axial dispersion on the feed concentration at z=0 [28]:

BC #1	$C(z = 0, t) = C_0 + \dfrac{D_{ax}\varepsilon_L}{u} \left.\dfrac{\partial C}{\partial z}\right|_{z=0}$	(1.17.2)

The second boundary condition expresses that at the top of the column, there is no more adsorbent and the concentration is not modified [28]:

BC #2	$\left.\dfrac{\partial C}{\partial z}\right|_{z=L} = 0$	(1.17.3)

2.7.2. *Solid phase*

In the solid phase, we will consider the concentration of protein that is binding to the adsorbent particles.

The mass balance with respect to the solid phase is described as follows:
Dispersion *in* at (z) + mass transfer to solid phase between (z) and (z+dz) = Accumulation in the solid phase between (z) and (z+dz) + Dispersion *out* at (z+dz)
There is no influence from the bulk flow because the proteins only move into the porous particle via a diffusion process.

In a mathematical manner:

$$-D_s A \frac{\partial q}{\partial z}\bigg|_z + \frac{3k_f \varepsilon_s}{R_p}\left(C - C_f\right)Adz = \varepsilon_s \frac{\partial q}{\partial t} Adz - D_s A \frac{\partial q}{\partial z}\bigg|_{z+dz} \qquad (1.18)$$

Rearranging (3)gives:

$$\varepsilon_s \frac{\partial q}{\partial t} = Ds \frac{\partial^2 q}{\partial z^2}\bigg|_z + \frac{3k_f \varepsilon_s}{R_p}\left(C - C_f\right) \qquad (1.19)$$

At time t=o, there is no protein in the column, therefore:

$$q(z, t = o) \qquad (1.19.1)$$

At the top and bottom of the column, there is no adsorbent; therefore there cannot be any

adsorption of proteins. This leads to the following boundary conditions [14]:

BC #1	$\frac{\partial q}{\partial z}\bigg|_{z=0} = 0$	(1.19.2)
BC #2	$\frac{\partial q}{\partial z}\bigg|_{z=L} = 0$	(1.19.3)

The film mass transfer coefficient k_f can be calculated as a function of the bed void

fraction using the following correlation [27]. Re_p is the Reynolds particle number, Sc is

the Schmidt number and D_m the molecular diffusion coefficient of the protein considered.

$$k_f = \frac{D_m}{d_p}\left[2 + 1.5(1 - \varepsilon_L)\,Re_p^{1/2}\,Sc^{1/3}\right] \qquad (1.20)$$

The solid dispersion coefficient is given as a function of the superficial velocity [29]:

$$D_s = 0.04u^{1.8} \qquad (1.21)$$

2.7.3. Homogeneous diffusion model

The homogeneous diffusion model is used to explore the kinetics of protein adsorption inside the porous particle. Equation 1.22 describes the concentration of the protein as a function of the time and the particle radius. Inside the pore, only a diffusion process occurs. Due to the spherical geometry of the adsorbent particle, Equation 1.22 has the following expression where q_i is the total protein concentration in the solid phase. q_i is not only a function of the particle radius but also a function of the axial coordinate z.

$$\frac{\partial q_i}{\partial t} = \frac{D}{r^2}\left(\frac{\partial}{\partial r}\left(r^2\frac{\partial q_i}{\partial r}\right)\right)$$

(1.22)

The initial condition shows that the adsorbent is free of protein at time = 0 :

$$q_i(r,z,t=o)$$

(1.22.1)

The first boundary condition describes the symmetry of the adsorbent particle. The second expresses that the increase of the solid phase in the porous particle is due to the mass transfer at the surface. q being the average solid phase concentration at a certain coordinate z, this boundary condition can be written as follows:

$$4\pi R_p^2 D\frac{\partial q_i}{\partial r}\bigg|_{r=R,z} = \frac{4\pi R_p^3}{3}\frac{\partial q}{\partial t}\bigg|_z$$

(1.23.1)

Becoming:

$$\frac{\partial q_i}{\partial r}\bigg|_{r=R,z} = \frac{R_p}{3D}\frac{\partial q}{\partial t}\bigg|_z$$

(1.23.2)

Injecting (6-b) into (II), we obtain the following boundary conditions:

BC #1	$\frac{\partial q_i}{\partial r}\bigg|_{r=0,z} = 0$	(1.22.2)

| BC #2 | $$\left.\frac{\partial q_i}{\partial r}\right|_{r=Rp,z} = \frac{R_p D_s}{3 D \varepsilon_s} \left.\frac{\partial^2 q}{\partial z^2}\right|_z + \frac{k_f (C - C_f)}{D}$$ | (1.22.3) |

2.7.4. *Langmuir isotherm*

The adsorption isotherm will be modeled using a Langmuir type equation. The isotherm will be used to determine the protein concentration at the particle surface.

$$q(R_p,z) = \frac{q_m . C_f}{K_d + C_f}$$	(1.24)

Where q_m is the adsorption capacity and K_d the dissociation constant. $q(R_p,z)$ and C_f are the aqueous and adsorbed protein concentration in equilibrium.

Nomenclature:

$C_f(t)$: protein concentration at the particle surface (mg/ml)

$C(z,t)$: protein concentration in the liquid phase (mg/ml)

$q_i(z,t)$: particle adsorbed protein concentration (mg/ml)

$q(z,t)$: average solid phase protein concentration (mg/ml)

D_m : molecular diffusion coefficient of the protein considered (m²/s)

Dax : liquid phase dispersion coefficient (m²/s)

Ds : solid phase dispersion coefficient (m²/s)

ε_L : liquid void fraction in expanded bed (-)

ε_s : effective porosity of adsorbent for the considered protein (-)

R_p : particle radius (m)

A : surface area of the column (m²)

u : superficial velocity (m/s)

2.8. Zirconia based adsorbent

2.8.1. *Small high density adsorbent*

Commercially available adsorbent such as cross-linked agarose weighted by incorporating fine crystalline quartz (Streamline) are characterized by a large particle size (100-300 μm) and a low density (1.1-1.3 g/ml). The mobile phase flow velocity is limited by the low density making the use of viscous fluids very difficult. Although, the large particle diameter provides a higher terminal settling velocity according to Stokes' Equation 1.25, the intraparticle mass transfer resistance would be increased due to the lengthy diffusion path.

$$U_t = \frac{(\rho_p - \rho_l).d_p^2.g}{18\eta} \hspace{2cm} (1.25)$$

Where U_t is the terminal velocity, ρ_p and ρ_l are respectively the particle and liquid density, d_p is the particle diameter, η is the solution viscosity and g the acceleration due to gravity.

A way to overcome those problems is to use small highly dense adsorbent particles [31]. Moreover, high fluidization velocities can be achieved with smaller adsorbent particles leading to a more rapid protein adsorption. The expanded bed will also be more stable over a wider range of fluid densities and viscosities with reduced dispersion within the bed. The time scale for intraparticle diffusion is reduced without compromising the operating velocity.

Several high-density and small-sized adsorbent for expanded bed chromatography have been developed such as pellicular stainless steel beads [32], fluoride modified

zirconia supports [33], supermacroporous cross-linked cellulose [34] and mineral oxide gel composite [35].

2.8.2. *Fluoride modified zirconia adsorbent*

Adsorbent based on zirconia have excellent mechanical, thermal and chemical stability [33]. This allows the sterilization and the cleaning under harsh conditions which cannot be done with a lot of polymeric adsorbent.

The interaction with the proteins is mainly due to the Lewis Acid sites on the zirconia surface [36]. These sites will interact differently with different solutes and can lead to badly broadened peaks or irreversible adsorption of strongly interacting solutes. Those Lewis acid sites create an irreversible retention of the proteins by complexing with the carboxyl-containing side chains of aspartate and glutamate residues as shown in Figure 9. The adsorption of the protein can be weakened by introducing a strong Lewis base in the mobile phase [37]. Fluoride interacts strongly with these hard surface Lewis acid sites as it is a strong Lewis base and at appropriate concentration can prevent irreversible protein adsorption. When the fluoride concentration in the eluent suffices to nearly saturate the support's Lewis base adsorption isotherm, the residual ligand-exhange interactions between the surface and the protein results in well shaped peaks. The balance of cation-exchange and ligand-exchange character of the support formed by this adsorptive surface modification provides unique chromatographic selectivity for the separation of proteins [38]. The retention mechanism of proteins on Lewis base modified zirconia surfaces can be compared to that of calcium hydroxyapatite. Adding a strong

Lewis base such as Fluoride creates a biocompatible stationary phase of unique mixed-mode surface chemistry referred as "fluoride-modified zirconia" (FmZr) [36].

    The excellent thermal and chemical stability allow steam sterilization and repeated cleaning and depyrogenation using 0.25M NaOH.
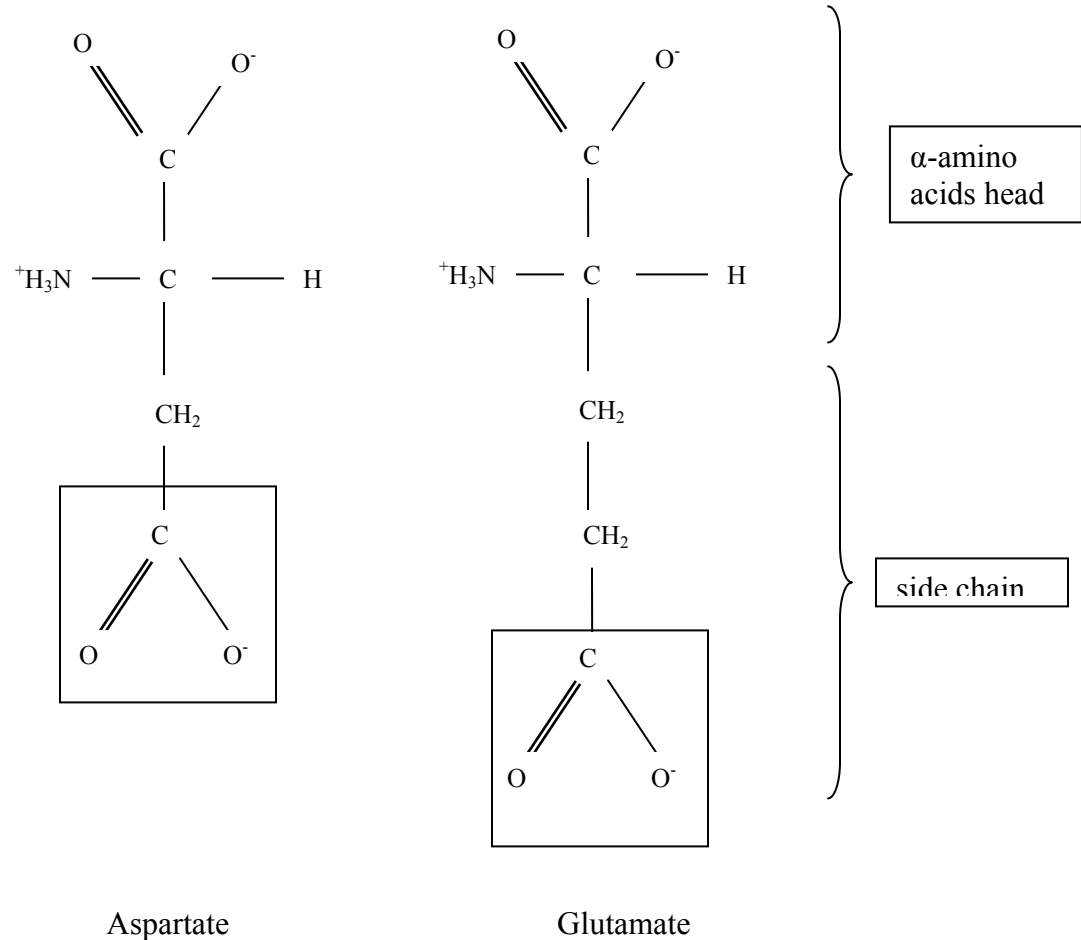
Figure 9 : Carboxyl containing side chains of Aspartate and Glutamate.

3. <u>Material and Methods</u>

3.1. *Column specifications*

We have purchased a STREAMLINE 25 column form Amersham-Bioscience which has a 25mm inner diameter (491 mm² of column cross section). The glass tube is 100mm long. The maximum operating pressure recommended is 1bar. The operating flow rates should be between 200 and 400cm/h (1-2 L/h).

3.1.1. *Experimental set-up*

In order to have either upward or downward flow coming from the same container, we used the apparatus described in Figure 10 where using valves V1 we can either obtain an upward flow as shown in Figure 10 or a downward flow as described in Figure 11. Being able to reverse the flow during the injection of the sample can be very useful because it occurs that for complex and viscous solutions, the bottom adaptor can be clogged by particulates. Pump 2 and valve V3 are used to operate the hydraulic adaptor. We also use a simple 4 way valve (V4) to change from one solution to another. This system allows us to use only two peristaltic pumps (Pump 1 and Pump 2). Valves V1 (SRV-4), V2 (SRV-3) and V3 (SRV-3) were purchased from Amersham Bio-Science. The UV detector is a UV-1 from Amersham Bio-Science. The UV signal was controlled and acquired by a computer using the UNICORN software. The cell had to be changed to a   S-2 flow cell (Amersham Bio-Science) that allows the use of higher flow rates. All the tubing used to connect the valves and the column were PTFE tubes with a 1.9mm inside diameter purchased from Amersham Bioscience.

3.1.2. *Operation of the column*

The first step is the *expansion step* where the bed is expanded to the desired height using the appropriate buffer. The bed is usually expanded in three steps: the velocity is gradually increased. For each flow speed, we need to wait for the bed to be stable. The bed is considered to be stable when only small circulatory movements of the adsorbent beads are observed. It usually takes 20-30 minutes to obtain a stable expanded bed. Other movements indicate turbulent flow or channeling. Large circular movements of the adsorbent beads in the upper part are usually due a bad vertical alignment. Channeling in the lower part indicates that either air is trapped under the adaptor plate or that the distributor may be partially clogged. A more analytical method is to measure the expansion of the bed or the number of theoretical plates as described in pages 20-23.

Once the bed has reached the desired expansion, the *sample feed is then injected* at the same flow rate. We usually stop the application when the UV signal reaches a plateau indicating that the adsorbent is saturated with protein. For viscous and complex feeds, we often need to back flush the lower adaptor to prevent any clogging. For viscous fluid, the expansion of the bed increases during the sample feed.

The *wash step* is performed, at the same velocity, to remove all the non-bound or weakly bound particulates or proteins. In order to perform a good clarification, concentration and initial purification, the particulate removal is a crucial step. Washing is performed until the UV signal returns to the base line. It is performed in expanded bed mode at the same flow rate as during the feed and expansion using the same expansion buffer. It usually takes 15-20 sedimented bed volumes to achieve an efficient wash.

The next step is the *elution* which can either be performed in expanded bed mode (usually when the feed is viscous and when channeling appeared during the sample application) or in a packed bed mode. For the packed bed option, we let the bed settle and then lower the adaptor to the surface of the sedimented bed. The elution is then performed with a downward flow. In order not to elute all the proteins at the same time, we use different solutions that have different sodium chloride concentration. The proteins that are more strongly bound will require a higher NaCl concentration to be eluted than weakly bound ones.

For complex solutions, some components cannot be removed during the elution step. To achieve a complete removal, a *cleaning in place (CIP)* procedure is required to restore the chemical and hydraulic properties of the adsorbent. This can also be used as a decontamination of the column to get rid of the biological hazard. CIP is a crucial step to ensure a long working life and therefore a decrease of the cost. CIP is usually performed at a very small velocity (30-100 cm/h). The contact time for an efficient CIP is 5-6 hours. The chemicals mainly used are: NaOH, Urea, HCl, Isopropanol 30% or Ethanol 70% [15].

Once the adsorbent is cleaned, to prevent any contamination, the column is filled with ethanol 20% for storage inside the column [15].
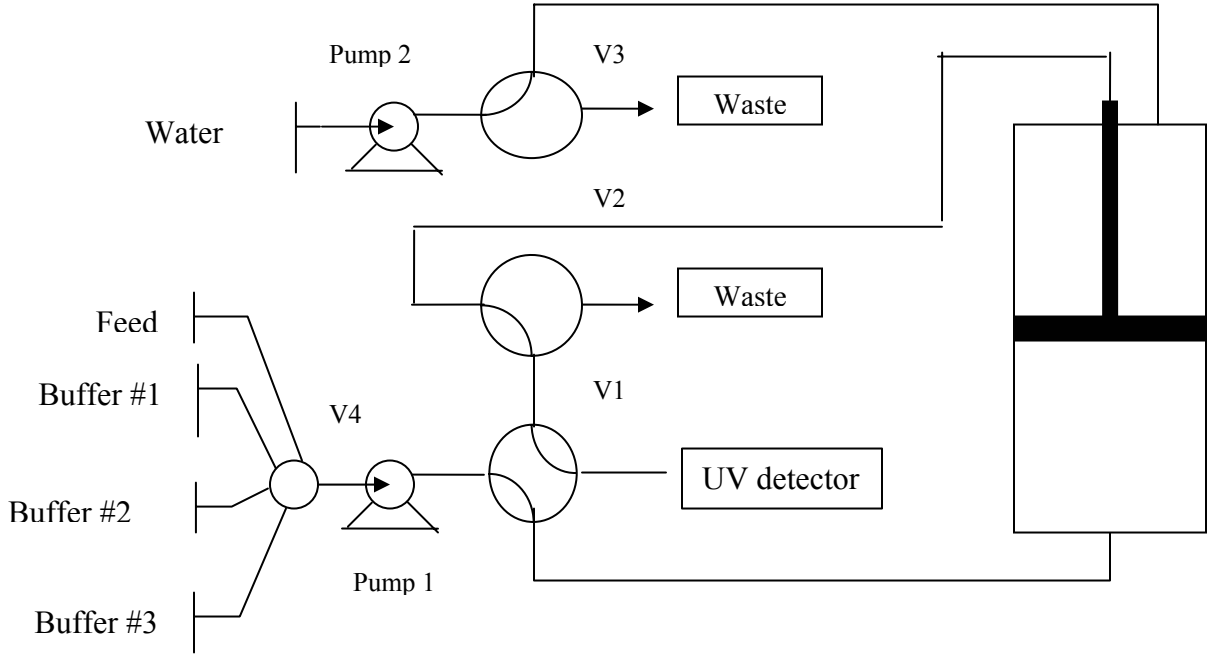
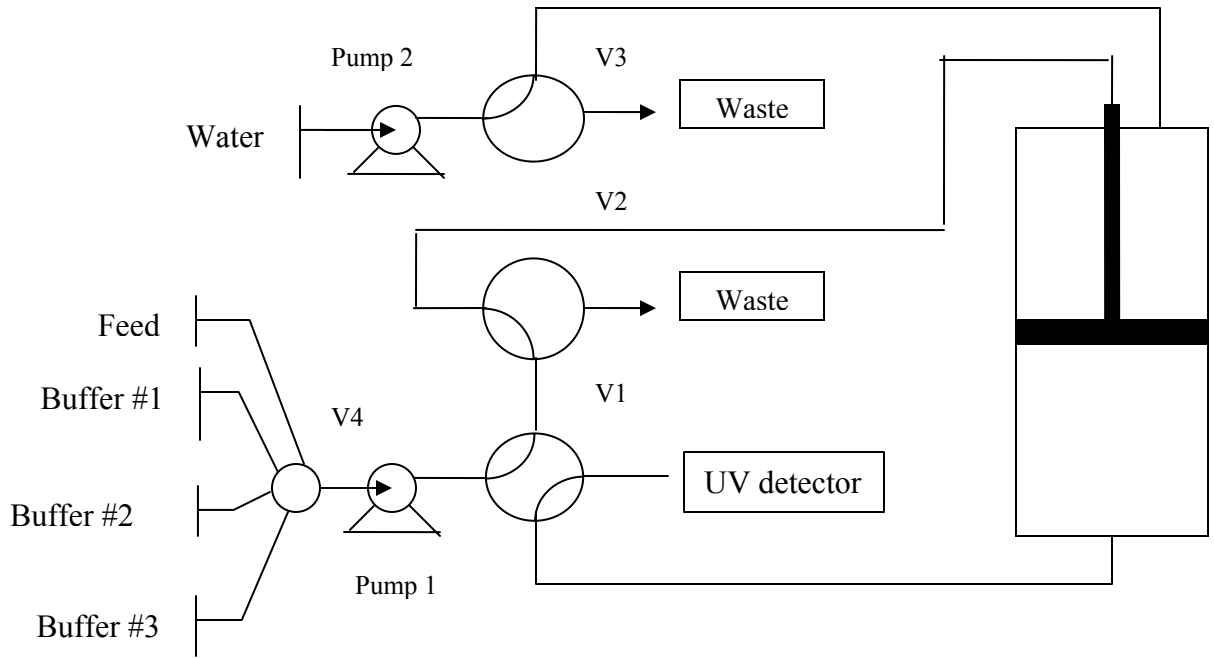**Figure 10 : Upward flow with fixed upper adaptor, used during expansion, feed, elution in expanded mode and CIP.**

Figure 11 : Downward flow with fixed upper adaptor, used for elution in packed bed mode.

3.2. Adsorbent used during experiments

3.2.1. *Streamline DEAE*

Various adsorbents differ in variables such as the chemistry of the functional group, the pore diameter and the charge density. The type of adsorbent used is a weak anion exchanger called DEAE (diethylaminoethyl). It is a "weak anion exchanger" because is has its maximum capacity at a certain pH where it maintains charge; whereas "strong anion exchanger" keep their charge over a wider pH range. Different kinds of matrices are available such as cellulose, sephacel (spherical cellulose beads), sephadex (dextran beads), agarose, synthetic-polymer (trisacryl) [9].

The adsorbent used in the expanded bed column is a Streamline DEAE manufactured by Amersham Bioscience. The base matrix is a highly cross-linked beaded agarose derivate based on 6% agarose [16]. The density of the matrix is increased by including an inert core in order to obtain a stable expansion of the bed. The macrostructure of the agarose is composed of polysaccharide chains arranged in bundles that are further strengthened by inter-chain cross-linking. Agarose-based matrices also have the advantage for their low-specific adsorption of macromolecules.

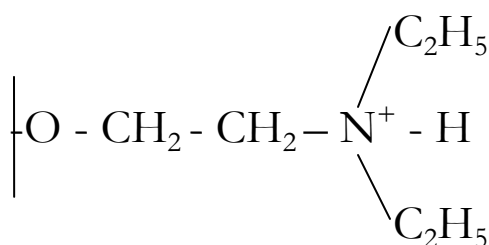The ligand attached to the matrix with the epoxy chemistry is as shown in Figure 12.

$$O - CH_2 - CH_2 - N^+ - H \begin{cases} C_2H_5 \\ \\ C_2H_5 \end{cases}$$

Figure 12 : Structure of coupled ligand on DEAE adsorbent.

The porosities of the base matrices and the coupling densities of the ligand attached provide a high binding capacity for protein adsorption. The number of ligand groups that are charged varies with the pH. This adsorbent maintains consistently high capacities over the pH range of 2-9 [16].

The high stability of this product allows cleaning in place under harsh conditions. The protocol used to clean and sanitize the adsorbent is described in Appendix 1.

Table 2 : Characteristics of Streamline DEAE adsorbent

Characteristics	**Streamline DEAE**
Total Ionic Capacity (mmol/ml gel)	0.13 – 0.21
Particle size range (μm)	100 – 300
Mean particle size (μm)	200
Mean particle density (μm)	1.2
Porosity	$4*10^6$ Daltons (globular proteins)
Matrix	Macroporous, cross-linked agarose, 6% containing crystalline quartz core material.
pH stability	2 – 13
Binding capacity (mg/ml gel)	40
Storage	20 % Ethanol

3.3. Chicken egg-white

3.3.1. *Buffer*

The buffer used for all the experiments was a 50mM Tris buffer of pH 7.5. The ionic strength of the buffer needs to be high enough to loose the particle-particle electrostatic interactions and therefore ensure a good expansion of the bed but it also needs to be relatively low not to interfere with the elution process. As the adsorbent used was a anion-exchange, the Cl⁻ ions contained in the buffer will be used as the counter ions for the adsorbent.

All the proteins that have an isoelectric point greater than the pH of the buffer, 7.5, will not bind to the DEAE adsorbent.

3.3.2. *Chicken egg solution*

The chicken egg white needs to be diluted, here is the procedure used to prepare the sample:

- Separate the chicken egg white from the yolk

- Dilute with 3 egg white volume with Tris Buffer 50mM pH 7.5

- Add NaCl to reach 0.1M concentration

- Add β-mercaptoethanol to reach a 10mM concentration

The solution is then gently stirred during 3 hours, filtered and left overnight in the fridge a 4°C. When adding the buffer solution, precipitate appears (presumably ovomucin). Even though adding NaCl allows us to get rid of some of the precipitate, we still need to filter the solution to prevent solid particles from plugging the distributor.

3.3.3. *Elution of BSA*

In order to find the exact concentration of NaCl needed to elute BSA, we used a packed bed column: a weak anion exchange DEAE sepharose 1mL column from Amersham Bioscience. This adsorbent contains the same reactive group (DEAE) as the one used in the expanded bed column.

This column is being controlled by a FPLC (fast protein liquid chromatography) system from Amersham Bioscience. This automated system consisted of two peristaltic pumps (P500), motor valves and a UV detector. All of these were calibrated and controlled by a computer using the UNICORN software. Using packed bed column allows us to use small volume and therefore to reduce cost. One experiment (equilibration-sample application-elution-cleaning) can be run in an hour and a half which is very small compared to the expanded bed (6-8h). Moreover, it is very easy with this system to monitor the salt concentration: the software controls the two pumps (one contains the buffer and the other a "buffer + 1M NaCl solution") to obtain the exact salt concentration by mixing those two solutions. We can either have a ramp or a step-like function for the NaCl concentration. We can therefore determine the minimal concentration of salt needed to elute a certain protein; this concentration will then be used when using the expanded bed column.

When using a ramp concentration profile (from 0 to 1M NaCl) we can estimate the concentration needed to elute BSA from a buffer solution. We then use a step response to determine the exact salt concentration.

3.4. Mathematical methods to solve the system

3.4.1. *Method of lines*

In order to solve Equations (I) and (II), a discretisation method called the method of lines [40]. The variable is only discretised upon the axial coordinate. The variable is no longer a function of time and axial coordinate but we convert this variable into a number N of time dependent variable. A partial differential equations is transformed into a set of differential algebraic equations as shown in Figure 13.
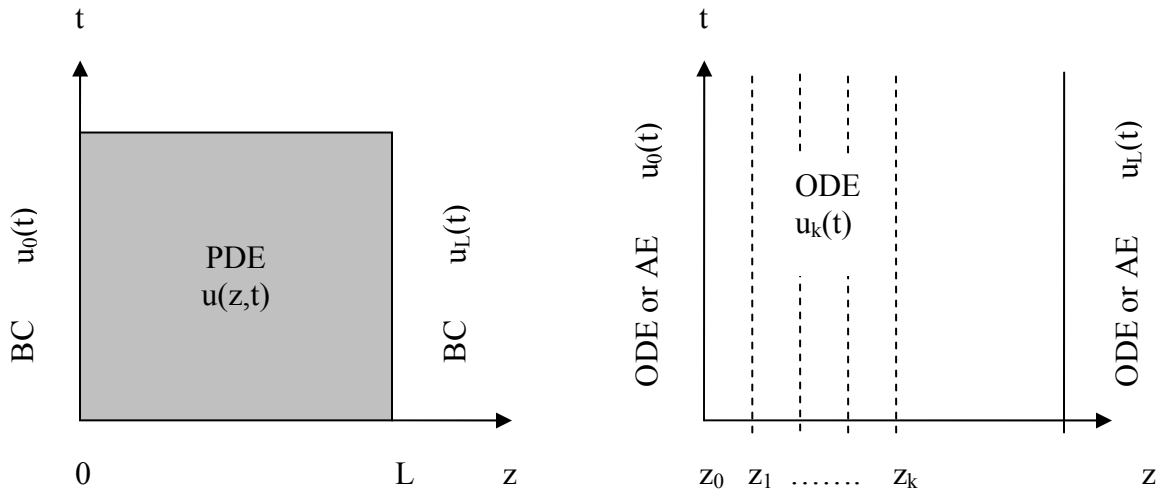
Figure 13 : Method of lines (MOL) approach for the transformation of a partial differential equation (PDE) and the related boundary conditions (BC) into ordinary and algebraic differential equations (ODE, AE) [40]

For example, if we consider Equation 2.1 and C(z,t) :

$$\frac{\partial C}{\partial t} = Dax \frac{\partial^2 C}{\partial z^2} - u \frac{\partial C}{\partial z} + \frac{3k_f \varepsilon_s}{\varepsilon_p R_p}\left(C - C_f\right)$$

(2.1)

Equation (I) then becomes a system of N equations:

$$\frac{\partial C_i}{\partial t} = Dax \frac{C_{i+1} - 2C_i + C_{i-1}}{h_x^2} - u \frac{C_{i+1} - C_{i-1}}{2h_x} + \frac{3k_f \varepsilon_s}{\varepsilon_p R_p} \left(C_i - C_{fi} \right)$$
(2.2)

Where h_x is the step size and i={1,N}

Equation 1.19 becomes :

$$\varepsilon_s \frac{\partial q}{\partial t} = Ds \frac{q_{i+1} - 2q_i + q_{i-1}}{h_x^2} + \frac{3k_f \varepsilon_s}{\varepsilon_p R_p} \left(C_i - C_{fi} \right)$$
(2.3)

This system of N first order differential equations can be solved using a Runge-Kutta of 4th order method:

$$Y_1 = f(x_i, y_i)$$

$$Y_2 = f(x_i + \frac{1}{2}h, y_i + \frac{1}{2}hY_1)$$

$$Y_3 = f(x_i + \frac{1}{2}h, y_i + \frac{1}{2}hY_2)$$

$$Y_4 = f(x_i + h, y_i + hY_3)$$

$$y_{i+1} = y_i + h(\frac{1}{6}Y_1 + \frac{1}{3}Y_2 + \frac{1}{3}Y_3 + \frac{1}{4}Y_4)$$

Where h is the time step.

3.5. FmZr adsorbent

3.5.1. *Synthesis*

The 20wt% suspended ZrO_2 particles used were purchased from Nyacol (Ashland, MA) and had a 1000Å nominal size. The procedure used to synthesize the porous zirconia particles was inspired by Robichaud and al [39].

The zirconia solution was centrifuged at 15,000g for 2.5 hours and the resulting cake was resuspended in pH 3 nitric acid to obtain a 45 wt% concentrated solution. Resuspension was carried out at room temperature in a shaking bath for 12-15 hours.

The experiments were carried out in a cylindrical glass vessel of 15 cm diameter. It was initially filled with a 1:1 ration volume of peanut oil and oleyl alcohol. The peanut oil and the oleyl oil were purchased from Sigma Inc. The emulsion was agitated with a centered 7cm diameter, 3 bladed propeller-type impeller rotating at a fixed speed just slow enough to avoid vortices. The oil-oleyl alcohol mixture was preheated to 95°C. The initial depth of emulsion was 3.5 cm.

The aqueous stream consists of the previously concentrated zirconia solution and the oil phase stream consists of the peanut and alcohol mixture. These streams were combined at room temperature at a 1:3 sol:oil ratio and the aqueous-oil dispersion was created using an in-line mixer of 0.5 cm inside diameter. The pumping was accomplished using a peristaltic pump. The addition of the sol-oil dispersion at room temperature causes the batch temperature to drop. The total volume will reach 700 ml (4cm of height). The agitation is increased but still avoiding vortices. The temperature increased to a steady-state temperature of 90°C after about 25 minutes, and the heating and stirring was continued in order to remove water from the sol droplets. As the water is eliminated, the

sol droplets densify and the droplets aggregate to form solid particles. The particles are considered stable when the largest ones remain intact without breaking after washing with isopropanol. The batch time is approximately 60 minutes. After this time, the batch is allowed to settle for 10 minutes. After decanting the oil, the particles are resuspended in five times in 200mL isopropanol. The particles are each time filtered under vacuum of a Buchner funnel. Finally, the particle are rinsed with isopropanol and dried under vacuum for 1 hour. The particles are then heated for 2 hours at 100°C to drive off water and isopropanol, followed by 2 hours at 375°C to burn remaining organics and 6 hours at 750°C to burn off surface carbon and nitrogen. The particles are finally sintered for 3 hours at 900°C to improve their mechanical strength.

The particles were then sieved to select the particles with a diameter between 50 and 100μm. The desired particles are then washed with 0.5M NaOH and 0.5M nitric acid to establish a consistent surface chemistry to prepare for chromatographic use. The base and acid wash is completed by adding the particles to enough carbonate-free double-distilled water to saturate and cover the particles. The water and particle are sonicated to eliminate air from the particles pores. The supernatant is removed and the particles are washed with 0.5M NaOH on a shaker table overnight. The particles are then washed with copious amount of water and dried under vacuum at 100°C for 8 hours. The particles are sieved again to determine the size distribution.

4. <u>Results and Discussions</u>

4.1. <u>Bed characteristics</u>

4.1.1. <u>Bed expansion</u>

The study of the bed expansion was carried out using pH 7.5 Tris-Buffer with different sedimented bed height. The results on Figure 14 were obtained with a diffusion plate composed of six 1mm diameter holes. Those results are in agreement with those found in the literature [15,40].
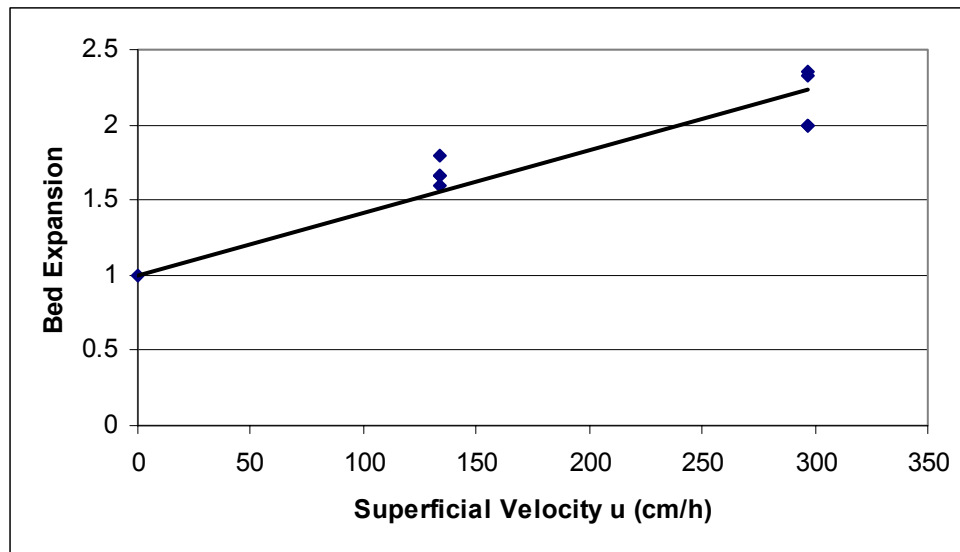

Figure 14 : Bed Expansion α for Streamline DEAE (1mm holes)

4.1.2. <u>Number of theoretical plates</u>

The number of theoretical plates N was calculated using the short cut method as described in "Materials and Methods". The tracer was a 1 % (V/V) acetone solution and the buffer used was pH 7.5 Tris-Buffer.

As shown on Fig 3.2, there is a great improvement in the number of theoretical plates when using a distributor plate with smaller holes in the bottom adaptor. The plate was composed of six 0.5 mm holes positioned in a hexagonal manner as shown on Fig 3.3 Those results are in agreement with Nayak and A.L. [40] who worked with macroporous crosslinked hydoxyethyl methacrylate-ethylene dimethacrylate copolymeric beads. Our result show that smaller holes create a lower pressure drop in the column and therefore, the expanded bed is more stable and offers a better resolution.
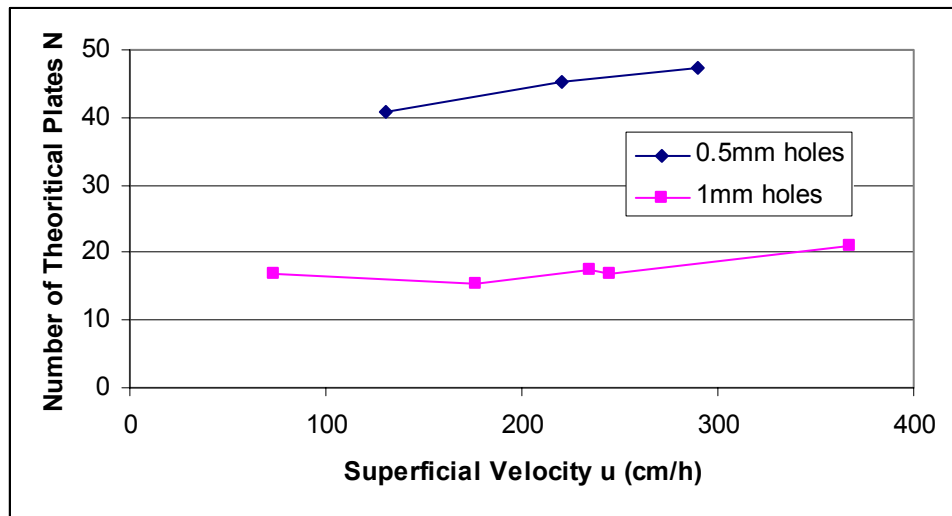

Figure 15 : Number of Theoretical Plates as a function of the Superficial Velocity

Figure 16 : Distributor stainless steal plate.

4.1.3. *Axial dispersion*

Figure 17 shows the effect of increasing interstitial fluid velocity on axial dispersion within expanded beds of STREAMLINE DEAE adsorbent. The clear tendency for D_{ax} to rise in response to increases in u was observed. We observed that with holes of smaller diameter, the axial dispersion coefficient is smaller than with wider holes.
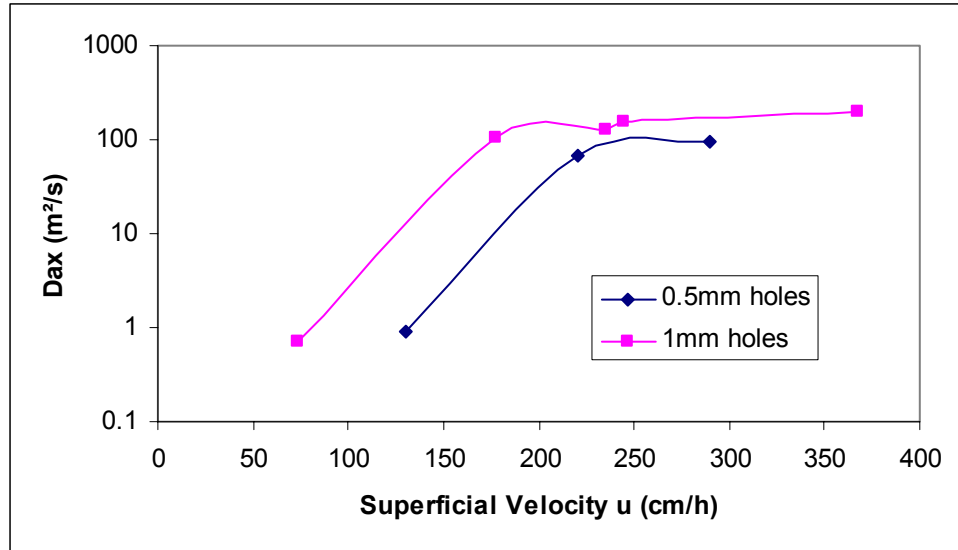
Figure 17 : Axial Dispersion coefficient as a function of the Superficial Velocity

Figure 17 shows the Bodenstein number Bo as a function of the superficial velocity. We need to be careful when analyzing those data because although the Bodenstein number represents the degree of axial mixing in the column, it may give a false impression of the efficiency of the expanded bed. According to Equation 1.2, the axial mixing coefficient, D_{ax}, depends on the flow velocity and the bed expansion height. Therefore, a higher Bo value may not mean a lower D_{ax}. The trend observed is in accordance with previous work [18,41] and we can conclude that the design of the column (size of the holes in the distributor plate) has a great influence on the performance of the column. All the values obtained for the Bodenstein number were near 40 or greater that there is no wall effect.
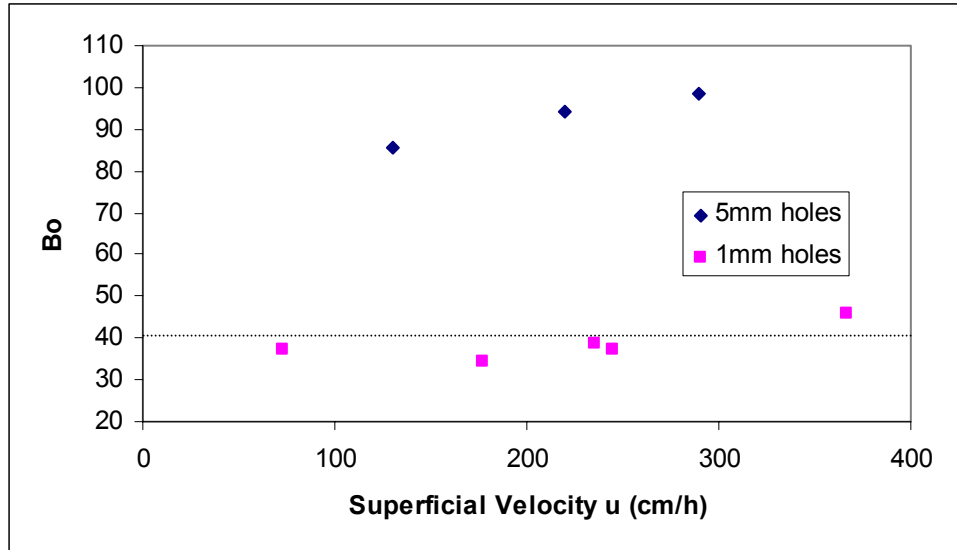
Figure 18 : The Bodenstein Number as a function of the Superficial Velocity.

4.1.4. *Richardson-Zaki equations*

We tried to confirm the validity of the Richardson-Zaki equation to predict the expanded bed height. By plotting LOG(ε) as a function of LOG(u) for the 1mm diameter hole distributor plate, we could determine the bed expansion index n as well as the terminal velocity according to Equation 1.8. Figure 19 shows the results obtained. The results are summarized in Table 3. We can conclude that the Richardsson-Zaki correlations are not suitable for predicting the fluidization behavior (e.g. height of the expanded bed H) of our experimental set-up.

Table 3 : Richardson-Zaki Method.

Diameter range (μm)	Mean Diameter (μm)	Particle density (mg/ml)	Ut from Stokes (cm/h)	Mean Ut (cm/h)
70-300 [11]	143	1.15	145-2675	605

Ho is considered to be 4.5cm

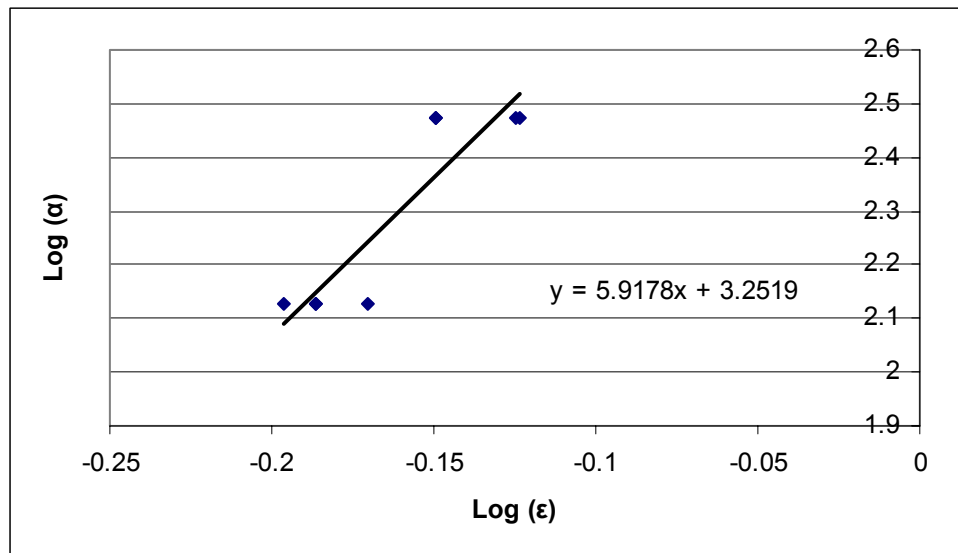|	Richardson - Zaki		Experimental		
Superficial Velocity (cm/h)	H (cm)	n	H (cm)	n	Ut (cm/h)
134	5.3	5.11	7.5	5.9	1780
297	7.4		9		

Figure 19 : Determination of the bed expansion index and the terminal velocity.

4.1.5. *Breakthrough curves*

Breakthrough curves were performed with a 0.5mg/ml solution of BSA in Tris-HCl buffer 50mM (pH 7.5) at various flowrates. Figure 20 shows the similitude between

the two curves and that the adsorbent is saturated in protein sooner when the linear velocity in the column is increased.
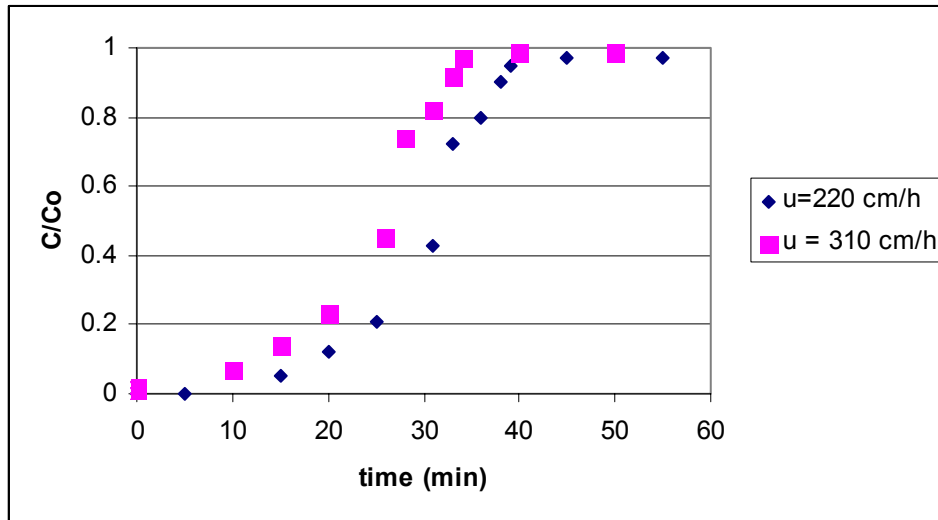

Figure 20 : Breakthrough curves for BSA at different linear velocities.

Using the equations described previously, the dynamic binding capacity was determined to be 34.5mg of BSA / ml of adsorbent at a linear velocity of 220cm/h. The calculation reveals that the flowrate has little effect on the DBC. For a linear velocity of 310 cm/h, the DBC was 32 5mg of BSA / ml of adsorbent.

4.1.6. *Effect of viscosity on the dynamic binding capacity*

Solutions of 0.1 M BSA in Tris HCl Buffer (50mM and pH 7.5) were used to obtain breakthrough curves. To increase the viscosity of the solute, glycerol was added to the solute. The dynamic binding capacity was found to be equal to 34.5 mg/ml of adsorbent. We tried to increase the viscosity from 1 cp to 10 cp (0% to 60% w/w glycerol) but the bed could not sustain viscosity higher than 3 cp (40% glycerol) : the adsorbent would then aggregate and channels would appear in the adsorbent making

adsorption impossible. Figure 21 shows a great decrease in protein adsorption when the viscosity is higher than 1.5 cp. We can assume that after 1.5 cp, channeling occurs in the bed but cannot be seen from the outside. When the channeling increases, more and more proteins are flushed out of the column without being adsorbed; the DBC therefore decreases.
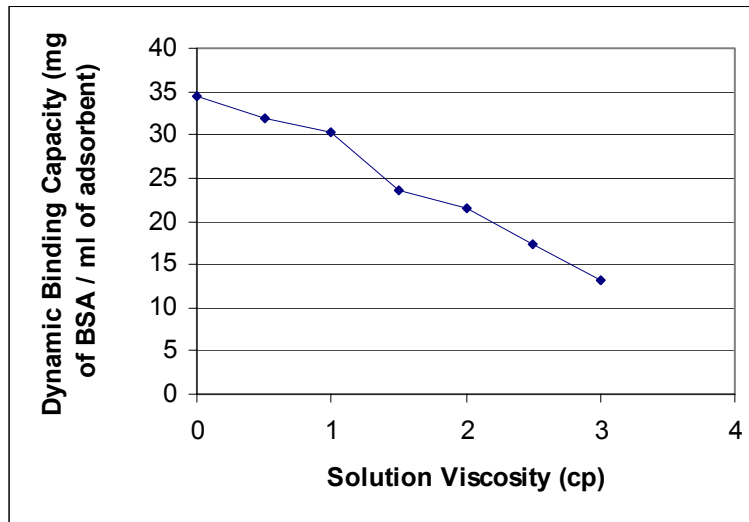

Figure 21 : Evolution of the Dynamic Binding Capacity with the solution viscosity.

4.2. BSA purification

4.2.1. *Determination of the Langmuir isotherm*

Bovine serum albumin was used as a model protein to determine the adsorption characteristics of the Streamline DEAE adsorbent. A 0.1 ml solution of drained adsorbent was added to 10 ml of BSA of different concentrations. The buffer used to dilute the BSA was the same as described in Appendix 2 : 0.05mg/l of Tris-HCl buffer (pH 7.5). After 6 hours in a shaking bath at room temperature, the mixture was let to settle and the supernatant was analyzed using the UV detector to determine the protein concentration. We could therefore calculate the mass of BSA that had been adsorbed by the adsorbent. This experiment was used to determine the Langmuir isotherm parameters.
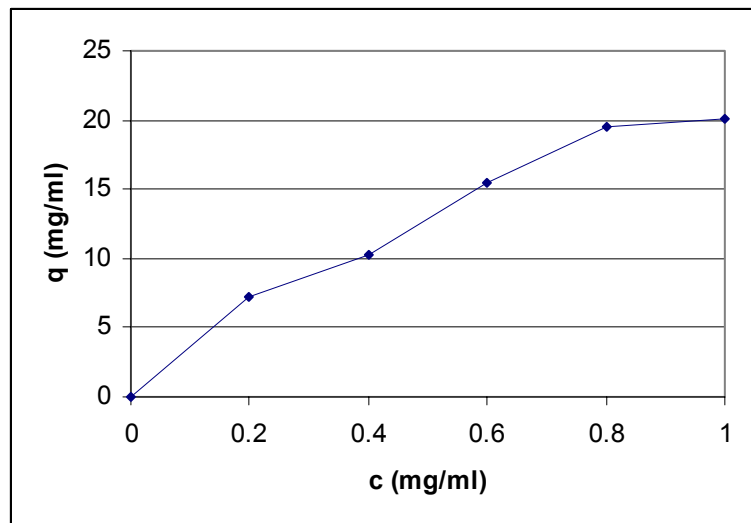

Figure 22 : Adsorption Isotherm of BSA on Streamline DEAE

When plotting $1/q$ as a function of $1/c$, we could determine the adsorption capacity q_m and the dissociation constant K_d.
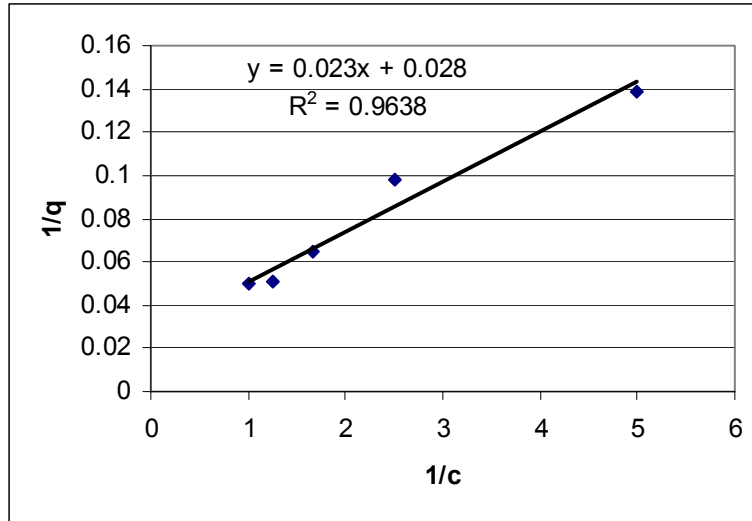
Figure 23 : Determination of the Langmuir parameters.

K_d was calculated to be 0.82 mg/ml and q_m to be 35.71 mg/ml.

4.2.2. *Kinetic parameters of the adsorbent*

To determine the kinetics parameters of the Streamline DEAE adsorbent, 0.5ml of drained adsorbent was mixed to 100 ml of 0.5mg/ml of BSA solution in Tris-HCl buffer 0.05 mg/ml (pH 7.5). The solution was continuously stirred and small sample (1 ml) were taken and rediluted 100 times for analysis using the UV detector. We could therefore obtain the evolution of the solute concentration as a function of time as shown of Figure 24.

The liquid film mass transfer coefficient for the batch adsorption system k_f was estimated using the following equation:

$$k_f = \frac{2D_m}{d_p} + 0.31 \left(\frac{\mu}{\rho D_m} \right)^{-2/3} \left(\frac{\Delta\rho}{\rho^2} \mu g \right)^{1/3}$$	(3.1)
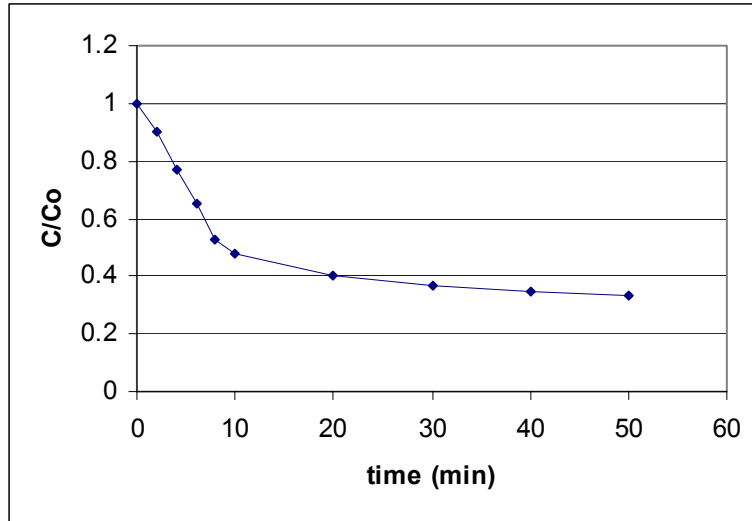
Figure 24 : Kinetics of BSA adsorption to Streamline DEAE

The liquid mass transfer was determined to be $24.2.10^{-6}$ m/s.

4.2.3. *Packed-bed column*

The packed-bed experiments were carried out using a 1 ml HiTrap DEAE Sepharose Fast Flow column purchased from AmershamBioscience. Figure 25 shows the UV signal at the output of the column for two chicken egg solutions. Those solutions were prepared as described on page 43 but we did not add the 0.1M NaCl and we added 0.5mg/ml of BSA in one of them. The solutions were filtrated under vacuum and were then injected into the column.
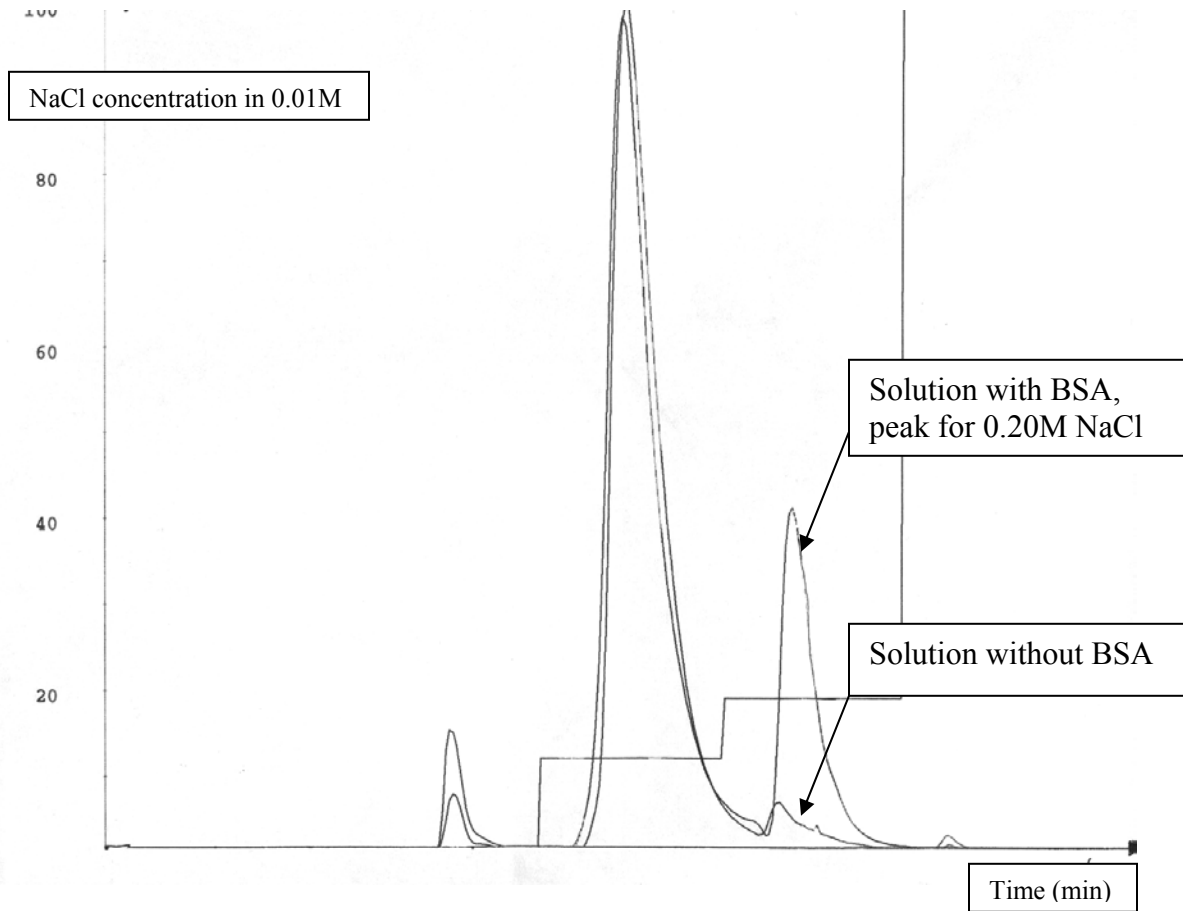
Figure 25 : Determination of the minimal NaCl concentration needed to elute BSA.

I should apologize for the poor quality of the picture but our system is very old and it only works with needle printers and the result is not very satisfying. In this experiment the time is not an issue and was not indicated on Figure 25.

We still could determine that the minimum concentration of NaCl needed to elute BSA was 0.2M. As shown on Figure 25, there is a small peak for the chicken egg white solution without BSA. Therefore our separation is not optimized; a second separation may be needed to separate the components in this peak.

4.2.4. *Expanded-bed column*

Knowing the concentration needed to elute BSA, we carried out experiments to test rather viscous chicken egg white solutions. The solutions were prepared as described in page 43; the BSA concentration was 0.5mg/ml.

Once the bed was fully expanded at the fluid velocity of 300 cm/h, the egg sample was injected until the UV signal reached a plateau where the feed stream was switched to the expansion buffer (ph 7.5 Tris-Buffer) in order to elute non binding proteins, and debris ; until the UV signal went back to the baseline. This step was the washing step. The first elution was performed using a 0.5M NaCl, a large peak was observed. Once the signal was back to the baseline, the second elution was performed using a 0.1M NaCl solution and as the egg solution already had a 0.1M slat concentration, the BSA peak was eluted. The last peak was obtained with a salt concentration of 0.9M NaCl.

We can observe on Figure 26 that the BSA elution peak is not pure : a peak is present for the solution without BSA. An analysis on the peak area and a more precise purification using packed bed column and small volume injected showed that the yeld for BSA was 85% but the purity would only reach 57%. We can recover 85% of the BSA in the elution peak but the purity is very low.
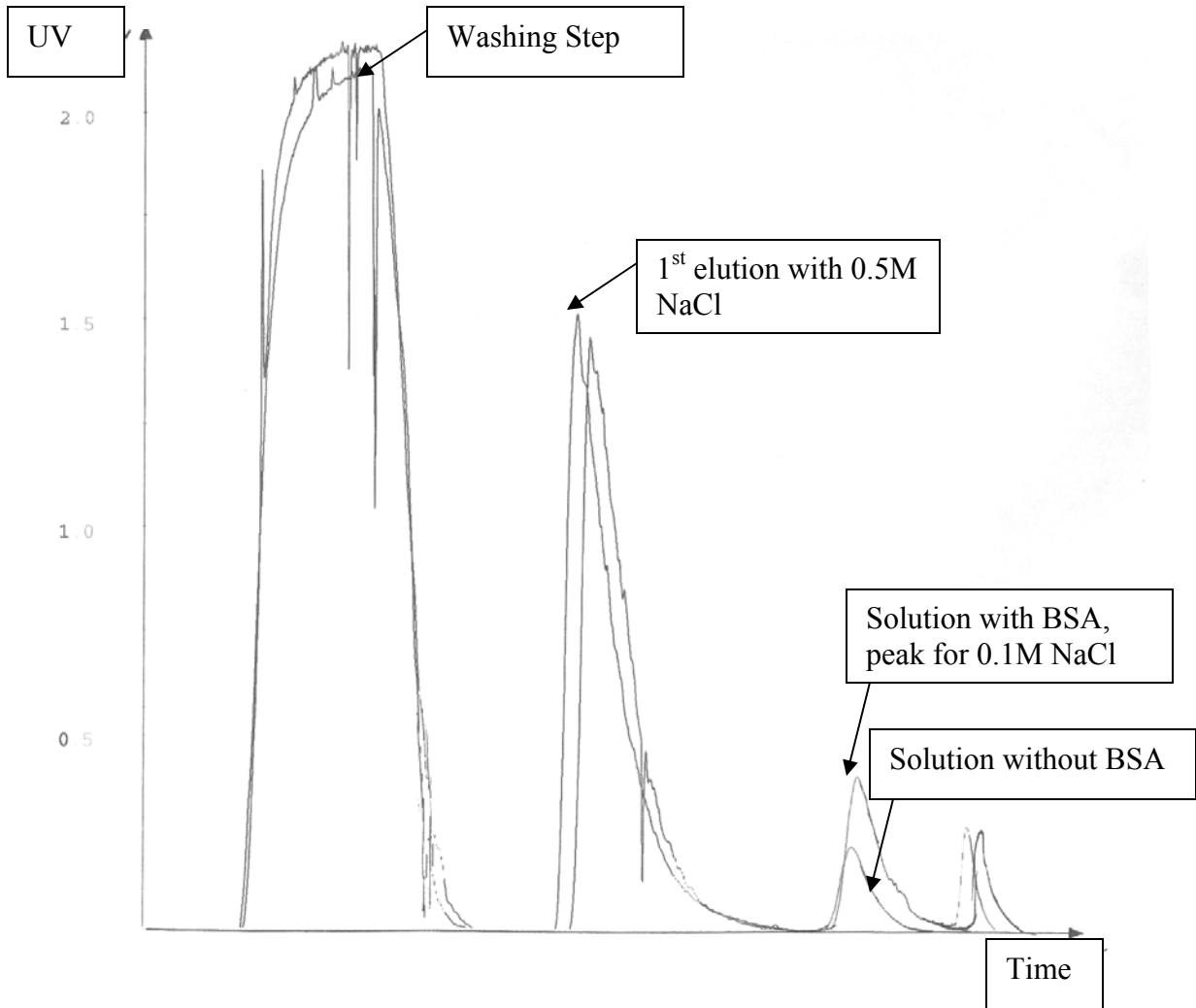
Figure 26 : Expanded bed operation with chicken egg white solution

4.3. FmZr adsorbent

4.3.1. *Results*

The major concern with this oil emulsion technique was the variability of the particle size with experiments conducted under identical conditions. The average particle size obtained for the three experiments was between 60 and 75 μm. Figure 27 shows the particle size distribution for one of the experiment where the mean diameter was 107 μm. The particles with a diameter smaller than 50 μm were not taken into account because if smaller, the particles would go through the net in the bottom adaptor.
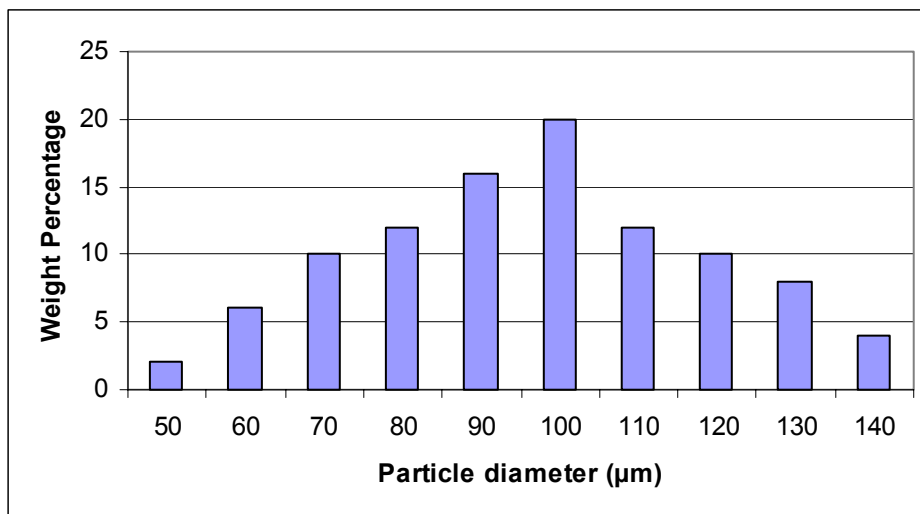
Figure 27 : Particule size distribution.

4.3.2. *Properties*

The only experiment we did with this adsorbent was to measure the adsorption of BSA on those zirconia particles. The results as shown on Figure 28 were not very good and the adsorbent synthesized would poorly adsorb BSA. We think that the cleaning process was not powerful enough to clean up the inside of the pores and allow the BSA to enter the particles. Experiments with this adsorbent were then stopped but further studies

should be carried on because theoretically, this type of adsorbent should allow better separation for complex solution.
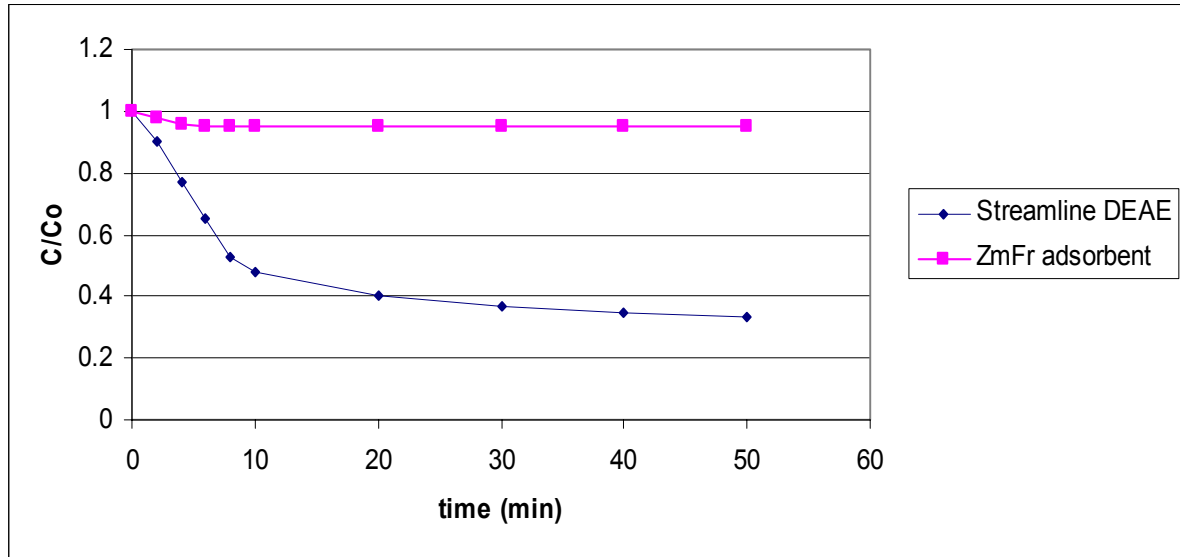
Figure 28 : adsorption comparison.

4.4. <u>Breakthrough curves simulations</u>

Those simulations were unsuccessful. The system would always be diverging. We tried to use the same value for the various constant used by Xiao-Dong Tong and al. [14} but without any success. We do think that the method of line may not provide a good discretisation of the system. Our code was working for other and simpler differential equation or system of differential equations but we think that this system is too stiff for a method of line combined with a Runge-Kutta method. Other numerical methods to solve differential equations should be investigated.

5. Conclusions

5.1. *Expanded bed chromatography*

This biosepartion process is very complicated to control. One of our main concerns was the channeling in the adsorbent: if channeling occurs, the sample is no longer in contact with protein free adsorbent and the separation resolution is therefore very small. Channeling often occurs when using very viscous and complex fluids such as chicken egg white solutions. When the viscosity is higher than 1.5cp, the adsorption is greatly decreased and it is impossible when the viscosity is higher than 3 cp. Channeling creates an early breakthrough for the sample. Often, with those solutions, the adsorbent had the tendency to get clogged and will not fully expand but become a solid mass that would be pushed towards the upper adaptor. In that case, the pressure inside the column tended to increase quickly and the risk of breaking the column was high. This solid mass would only let a small amount liquid to pass through.

When those situations occurred, a long (8 hours) cleaning in place procedure is needed to retrieve the chemical and physical properties of the adsorbent. After every chicken egg white run, this CIP procedure was needed (Appendix 1).

When using such complex fluids, we needed to back-flush the bottom adaptor so that it would not get clogged, therefore creating a uneven plug flow profile in the column. We could actually see the areas of the distributor that were clogged by judging by the behavior of the adsorbent particle

5.2. <u>Column design</u>

The reduction of the size of the holes showed promising results and we now need to keep on exploring the modifications we could do to improve the bottom distributor, especially to improve the cleaning process.　But as mentioned previously, even 1mm diameter holes get clogged so we tend to think that smaller holes will get clogged even faster.

5.3. *<u>Chicken egg white purification</u>*

The results obtained with the DEAE Streamline adsorbent are promising. We can actually extract BSA from a viscous and only diluted three times. Expanded bed can be used as a first step but not as a final purification. The yield was 85% but the purity would only reach 57 %.

5.4. *<u>Perspectives</u>*

We now know that some other components are eluted at the same time as BSA but we need to eliminate those bi-products.

The zirconia adsorbent is theoretically speaking very promising but a lack of knowledge in particle preparation could not provide us with an adsorbent capable of adsorbing BSA. The process has to be improved in order to obtain a better reproducibility and to improve the cleaning process of those particles.

Nomenclature

C_0: protein concentration in the feed solution (mg/ml)

u: the flow rate (ml/h)

V_d: the dead volume between the height of the bed and the upper adaptor (ml)

V_s: the sedimented bed volume (ml of adsorbent)

$C_f(t)$: protein concentration at the particle surface (mg/ml)

$C(z,t)$: protein concentration in the liquid phase (mg/ml)

$q_i(z,t)$: particle adsorbed protein concentration (mg/ml)

$q(z,t)$: average solid phase protein concentration (mg/ml)

D_m : molecular diffusion coefficient of the protein considered (m²/s)

Dax : liquid phase dispersion coefficient (m²/s)

Ds : solid phase dispersion coefficient (m²/s)

ε_L : liquid void fraction in expanded bed (-)

ε_s : effective porosity of adsorbent for the considered protein (-)

R_p : particle radius (m)

A : surface area of the column (m²)

u : superficial velocity (m/s)

k_f : film mass transfer coefficient (m/s)

Appendix 1

Cleaning in Place (CIP), sanitization and sterilization:

This is the procedure used to clean the Streamline DEAE adsorbent.

1/ 0.5M NaOH + 1M NaCl at a low flow velocity (30-60 cm/h) during at least 4 hours.

2/ Wash Buffer (50mM Tris pH 7.5) at 100 cm/h for 4 sedimented bed volumes

3/ 30% Isopropanol at 100 cm/h for 4 sedimented bed volumes

4/ 70% Ethanol at 100 cm/h for 4 sedimented bed volumes

5/ 25% Acetic Acid at 100 cm/h for 4 sedimented bed volumes

6/ Wash Buffer (50mM Tris pH 7.5) at 70-100 cm/h for 7-10 sedimented bed volumes

The adsorbent then is stored inside the column in a 20% Ethanol solution.

Appendix 2

Tris Buffe used during experiments:

Tris HCl : 2.16g

Tris Base : 1.62g

The total concentration is 50mM and the pH is 7.5. Working at pH 7.5 lead all the proteins with a pI>7.5 not to bind to the DEAE adsorbent.

Appendix 3

Example of calculation to determine the expanded bed characteristics:

We are going to explain how we obtain the results for the first line of Table 4.

Table 4 : Calculation of expanded bed characteristics

u(cm/h)	Ho (cm)	H (cm)	N	tr (min)	$\sigma_{\theta\,(min)}$	Bo
73	5.3	8.5	16.91	25.50	6.2	37.43
177	5.3	6.5	15.32	21.14	5.4	34.22
235	5.3	7.4	17.5	17.99	4.3	38.62
245	5.3	9.9	16.75	15.14	3.7	37.11
367	5.3	10.2	21.06	9.64	2.1	45.79

ε	α	Dax (cm²/s)	10E6 * Dax(m²/s)	HETP
0.637106	1.603774	0.00722783	7.23E-01	0.502661
0.525446	1.226415	1.06641722	1.07E+02	0.424282
0.583162	1.396226	1.2869057	1.29E+02	0.422857
0.688424	1.867925	1.58235134	1.58E+02	0.591045
0.697588	1.924528	1.95319316	1.95E+02	0.48433

H_0 and H were measured on the column. This was made easy by the fact that the column is made of glass. The retention time and the variance were calculated using the chromatogram given by our UV detector. The software we had was not very powerful so but we could read the exact value of the UV signal and the exact time. Therefore we could measure the time when the signal value was 27.5%, 50% and 87.5% of its maximum value.

The number of plates N was determined using Equation 1.11:

$$N = 25.50^2/6.02^2 = 16.91 \text{ plates}$$

The Bodenstein number was calculated using Equation 1.3, but the variance was converted into a non dimensional variance by dividing the variance by the retention time:

$\sigma = 6.2/25.5 = 0.24$ and Bo = 37.43

The bed porosity was calculated as follow:

$\varepsilon = 1-(1-0.418)*H_0/H$ where 0.418 is the settled bed porosity.

We could then calculate the axial diffusion coefficient:

$D_{ax} = (73*8.5)/(0.637*37.43)*1/3600 = 0.072$

References

1. Harvey, A. J., Speksnijder, G., Baugh, L. R., Morris, J. A., and Ivarie, R., "Expression of exogenous protein in the egg white of transgenic chickens", Nature Biotechnol., 19, 396 (2002).

2. AviGenics, Inc. web page; http://www.avigenics.com, May, 2000.

3. Ohtani, W., Nawa, Y., Takeshima, K., Kamuro, H.,Kobayshi, K., and Ohmura, T., "Physiochemical and immunochemical properties of recombinant human serum albumin from Pichia pastoris", Analytical Biochem., 256, 56(1998)

4. Eckelbecker, L., "In search of the golden egg", Worcester Telegram and Gazette, p. E-1, March 5, 2000.

5. Rita d'Aquino, "Green Factories for Pharmaceuticals", CEP, 99,1 (2003)

6. Noda, M., Sumi, A., Ohmura, T., and Yokoyama, K., "Process for purifying recombinant human serum albumin", U. S. Patent 5,962,649, October, 1999.

7. Stadelman, W. J. and Cotterill, O. J., Eds., Egg Science and Technology, 4th Ed., Haworth Food Products Press, New York, 1995.

8. Awade, A. C. and Efstathiou, T., "Comaprison of three liquid chromatography methods for egg-white protein analysis", J. Chrom. B, 723, 69 (1999).

9. F. Birger Anspach, David Curbelo, Ralf Hartmann, Gunnar Garke and Wolf-Dieter Deckwer,"Expanded-bed chromatography in primary protein purification", Journal of Chromatography A, Volume 865, Issues 1-2, 31 December 1999, Pages 129-144

10. Xiao–Dong Tong and Yan Sun, "Nd–Fe–B alloy-densified agarose gel for expanded bed adsorption of proteins", Journal of Chromatography A, Volume 943, Issue 1, 11 January 2002, Pages 63-75

11. Ming, F., Howell, J., Acosta, F., and Hubble, J., "Study on separation of conalbumin and lysozyme from high concentration fresh egg white at high flow rates by a novel ion-exchanger", Biotechnol. Bioeng., 42, 1086, (1993).

12. Owen, R. O. and Chase, H. A., "Direct purification of lysozyme using continuous counter-current expanded bed adsorption", J. Chrom. A, 757, 41, (1997).

13. Wright, P.R., Muzzio, F.J. "Effect of solution viscosity and mass transfer on adsorption", Biotechnology Progress, 1998, Volume 14, pages 913-921

14. Xiao-Dong Tong, Xiao-Yan Dong and Yan Sun," Lysozyme adsorption and purification by expanded bed chromatography with a small-sized dense adsorbent",

Biochemical Engineering Journal, Volume 12, Issue 2, November 2002, Pages 117-124

15. Expanded bed adsorption; principles and methods, Amersham Pharmacia Biotech, (1997).

16. Robert Scopes, Protein Purification : Principles and Practice, Springer-Verlag, New-York, 1982

17. O. Levenspiel, Chemical Reaction Engineering, 3rd edition, Wiley, New York, 1999

18. Irini Theodossiou, H. David Elsner, Owen R. T. Thomas and Timothy J. Hobley," Fluidisation and dispersion behaviour of small high density pellicular expanded bed adsorbents", Journal of Chromatography A, Volume 964, Issues 1-2, 26 July 2002, Pages 77-89

19. Hojrth, Leijon, A.K. Barnsfild Frzej in G Subramanian (Ed.) Bisoseparation and bioprocesssing, Vol. 1, Wiley, Weinheim, 1998, p199, Chapter 9

20. F. Birger Anspach, David Curbelo, Ralf Hartmann, Gunnar Garke and Wolf-Dieter Deckwer, "Expanded-bed chromatography in primary protein purification", Journal of Chromatography A, Volume 865, Issues 1-2, 31 December 1999, Pages 129-144"

21. J. F. Richardson and W. N. Zaki," The sedimentation of a suspension of uniform spheres under conditions of viscous flow", Chemical Engineering Science, Volume 3, Issue 2, April 1954, Pages 65-73

22. Gerard M. S. Finette, Qi-Ming Mao and Milton T. W. Hearn, "Studies on the expansion characteristics of fluidised beds with silica-based adsorbents used in protein purification", Journal of Chromatography A, Volume 743, Issue 1, 30 August 1996, Pages 57-73

23. J. J. van Deemter, F. J. Zuiderweg and A. Klinkenberg, "Longitudinal diffusion and resistance to mass transfer as causes of nonideality in chromatography" Chemical Engineering Science, Volume 5, Issue 6, September 1956, Pages 271-289

24. Anita Pai, Shyamal Gondkar and Arvind Lali, "Enhanced performance of expanded bed chromatography on rigid superporous adsorbent matrix", Journal of Chromatography A, Volume 867, Issues 1-2, 21 January 2000, Pages 113-130

25. N. B. Afeyan, N. F. Gordon, I. Mazsaroff, L. Varady and S. P. FultonY. B. Yang and F. E. Regnier, "Flow-through particles for the high-performance liquid chromatographic separation of biomolecules": perfusion chromatography, Journal of Chromatography A, Volume 519, Issue 1, 19 October 1990, Pages 1-29

26. J.D. Seader, E.J. Henley, Separation Process Principles, Wiley, 1999

27. Fan, Yang, C.Y. Wen, "Mass transfer in Semifluidized beds and solid-sliquid systems", AICHEj, Voluime 6, 482, 1960

28. Pamela R. Wright and Benjamin J. Glasser, "Modeling Mass Transfer and Hydrodynamics in Fluidized-Bed Adsorption of Proteins", AIChE Journal, Volume 47, Issue 2, February 2001, Pages 474-488

29. Van der Meer, C.M.J.P Blanchards, J.A. Wesselingh, "Mixing of particles in liquid fluidized beds", Chem Eng Res Des, 62, 1989 , pages 214-222

30. Suzuki M., Kawazoe K., "Effective surface Diffusion coefficients of volatile organic solvents on activated carbon during adsorption from aqueous solution" J Chem.. Eng. Jpn, Volume 8, 1975, pages 379-386

31. Wright, P. R., F. J. Muzzio, and B. J. Glasser, "Effect of Resin Characteristics on Fluidized Bed Adsorption of Proteins", Biotechnol. Prog. 15, 932, (1999).

32. Eva Pålsson, Per-Erik Gustavsson and Per-Olof Larsson, "Pellicular expanded bed matrix suitable for high flow rates", Journal of Chromatography A, Volume 878, Issue 1, 5 May 2000, Pages 17-25

33. C. M. Griffith, J. Morris, M. Robichaud, M. J. Annen, A. V. McCormick and M. C. Flickinger, "Fluidization characteristics of and protein adsorption on fluoride-modified porous zirconium oxide particles", Journal of Chromatography A, Volume 776, Issue 2, 1 August 1997, Pages 179-195

34. Anita Pai, Shyamal Gondkar and Arvind Lali, "Enhanced performance of expanded bed chromatography on rigid superporous adsorbent matrix", Journal of Chromatography A, Volume 867, Issues 1-2, 21 January 2000, Pages 113-130

35. N. Voute, D. Bataille, P. Girot, « Characterization of very dense mineraloxide gel composites for fluidized bed adsorption of biomolecules" Bioseparations, Vol 8, 1999 , pages 121-129

36. J. A. BlackwellP. W. Carr, "Fluoride-modified zirconium oxide as a biocompatible stationary phase for high-performance liquid chromatography", Journal of Chromatography A, Volume 549, 1991, Pages 59-75

37. J. A. BlackwellP. W. Carr," Study of the fluoride adsorption characteristics of porous microparticulate zirconium oxide" Journal of Chromatography A, Volume 549, 1991, Pages 43-57

38. John A. BlackwellPeter W. Carr, " Ion- and ligand-exchange chromatography of proteins using porous zirconium oxide supports in organic and inorganic Lewis base

eluents", Journal of Chromatography A, Volume 596, Issue 1, 3 April 1992, Pages 27-41

39. Robichad MJ, Sathyagal AN, Carr Pw, McCornick AV, Flickinger MC, 1997, "An improved oil emulsion synthesis method for large porous zirconia particles for pascked bed of fluidized bed protein chromatography", Sep Sci Technol , Vol 32 , 1997 , pages 2547-2559

40. Deba Prasad Nayak, Surendra Ponrathnam and C. R. Rajan, "Macroporous copolymer matrix: IV. Expanded bed adsorption application", Journal of Chromatography A, Volume 922, Issues 1-2, 13 July 2001, Pages 63-76

41. Alex J. Harvey, Gordon Speksnijder, Larry R. Baugh, "Expressino of exogenous protein in the egg white of transgenic chickens", Nature Biotechnology, Volume 19, April 2002, pages 396-399.